



Dahms, D., Egli, M., Fabel, D. , Harbor, J., Brandová, D., de Castro Portes, R. and Christl, M. (2018) Revised Quaternary glacial succession and post-LGM recession, southern Wind River Range, Wyoming, USA. *Quaternary Science Reviews*, 192, pp. 167-184.(doi:[10.1016/j.quascirev.2018.05.020](https://doi.org/10.1016/j.quascirev.2018.05.020))

This is the author's final accepted version.

There may be differences between this version and the published version. You are advised to consult the publisher's version if you wish to cite from it.

<http://eprints.gla.ac.uk/163679/>

Deposited on: 25 July 2018

Enlighten – Research publications by members of the University of Glasgow
<http://eprints.gla.ac.uk>

1 **Revised Quaternary glacial succession and post-LGM recession,**
2 **southern Wind River Range, Wyoming, USA.**

3
4 Dennis Dahms^{1*}, Markus Egli², Derek Fabel³, Jon Harbor⁴,
5 Dagmar Brandova², Raquel de Castro Portes², Marcus Christl⁵

6
7
8 ¹Department of Geography, University of Northern Iowa, Cedar Falls, USA

9 ²Department of Geography, University of Zürich, CH-8057 Zürich, Switzerland

10 ³Scottish Universities Environmental Research Centre, University of Glasgow, Scotland, UK

11 ⁴Earth, Atmospheric, and Planetary Sciences, Purdue University, West Lafayette, IN, USA

12 ⁵Institute of Ion Beam Physics, ETH-Zürich, CH-8093 Zürich, Switzerland

13
14 **Declarations of interest: None**

15
16 *Corresponding author. Tele: +1 319.230.9980.

17 E-mail address: dennis.dahms@uni.edu

18
19 *Keywords:* Glacial succession, cosmogenic surface-exposure dating, Wind River Mountains,
20 Wyoming, deglaciation, Younger Dryas, Older Dryas, Temple Lake, Alice Lake.

21
22 **Abstract**

23 We present here a more complete cosmogenic chronology of Pleistocene glacial deposits for the
24 Wind River Range, Wyoming, USA. Fifty-one new and thirty-nine re-calculated ¹⁰Be and ²⁶Al
25 exposure ages from Sinks and North Fork canyons, Stough Basin, Cirque of the Towers and the
26 Temple Lake valley allow us to more tightly constrain the timing and sequence of glacial
27 alloformations in the southern portion of the range.

28 Moraines, diamicts and bedrock exposures here have previously been correlated with as many as
29 five Pleistocene and four Holocene glacial events. Exposure ages from Pleistocene alloformations
30 associated with trunk glaciers in Sinks Canyon and North Fork Canyon generally confirm earlier
31 age estimates. Cosmogenic radionuclide (CRN, ¹⁰Be and ²⁶Al) ages from moraines and striated
32 bedrock surfaces previously mapped as Pinedale correspond to MIS2, while boulder exposure
33 ages from moraines mapped as Bull Lake correspond generally to MIS5-MIS6. Geomorphic data
34 from a moraine previously mapped as Younger pre-Sacagawea Ridge appears to correspond most

35 closely to the Sacagawea Ridge glacial episode (MIS-16), but the uncertainty of a single ^{10}Be
36 exposure age suggests the unit could be as young as MIS-10 or as old as MIS-18. Boulders from a
37 diamict on Table Mountain previously reported as Older pre-Sacagawea Ridge yield two ^{10}Be
38 exposure ages that suggest the presence of Early Pleistocene glacial activity here possibly older
39 than $\sim 1\text{-}2\text{ Ma}$ ($>\text{MIS-30}$).

40 Bedrock exposure ages within Sinks Canyon suggest the Pinedale valley glacier had retreated from
41 the floor of Sinks Canyon to above PopoAgie Falls by $\sim 15.3\text{ ka}$. Cirque glaciers in Stough Basin
42 appear to have retreated behind their riegels by $\sim 16\text{ ka}$, which suggests the cirque glaciers were
43 decoupling across their riegels from the valley glaciers below at this time, prior to their readvance
44 to form Lateglacial moraines.

45 New ^{10}Be boulder exposure ages from moraines previously correlated to the Temple Lake and
46 Alice Lake allostratigraphic units in the cirques of Stough Basin and Cirque of the Towers show
47 general equivalence to the stadial event just prior to the onset of the Bølling interstadial (17.5-
48 14.7 ka) and to the Intra-Allerød Cold Period-Younger Dryas stadial phase (13.9-11.7 ka),
49 respectively. From this evidence, the Temple Lake Alloformation of the Wind River Mountains
50 now should correspond to the INTIMATE GS-2.1a (Oldest Dryas) stadial event while the Alice Lake
51 Alloformation should correspond to the INTIMATE GS-2 stadial (IACP-Younger Dryas). Thus, we
52 consider that evidence no longer exists for early- to mid-Holocene glacial events in the southern
53 Wind River Range.

54

55 **1. Introduction**

56 The U.S. Rocky Mountains contain numerous ranges with records of multiple Pleistocene glacial
57 episodes ([Richmond, 1986](#); [Dahms, 2004b](#); [Locke, 1990](#); [Locke and Smith, 2004](#); [Osborn and](#)
58 [Gerloff, 1997](#); [Pierce, 2004](#); [Pierce et al., 2018](#)). The Greater Yellowstone Ecosystem of Wyoming-
59 Montana-Idaho plays a central role in our understanding of North American alpine glacial history
60 as it contains many of the type localities used for our present understanding of the Pleistocene-
61 Holocene glacial succession in this region of the Rockies (e.g., [Richmond, 1986](#); [Dahms, 2004b](#);
62 [Dahms et al., 2010](#); [Pierce, 2004](#)). The Wind River Range (WRR) occupies the southern-most
63 portion of the Greater Yellowstone Geocosystem and, along with Yellowstone Park itself, is the

64 focus of much past and continuing research into the regional Pleistocene glacial succession
65 ([Blackwelder, 1915](#); [Richmond, 1948, 1964, 1965, 1973, 1986](#); [Richmond and Murphy, 1965,](#)
66 [1989](#); [Murphy and Richmond, 1965](#); [Mears, 1974](#), [Dahms, 2004a, b](#); [Dahms et al., 2010](#)).

67

68 1.1 Pleistocene Succession of the WRR

69 Glaciers in the Wind River Mountains have occupied all of the range's major alpine valleys. Using
70 the seminal works of [Blackwelder \(1915\)](#) and Love ([Mears, 1974](#)), [Richmond \(1965, 1986 and](#)
71 [references therein](#)) presented morphostratigraphic evidence from the Bull Lake Type Area (BLTA)
72 that identified a series of moraine, outwash and lake deposits at Cedar Ridge corresponding to five
73 purported early-to-late Pleistocene glacial periods [from youngest: Pinedale - Bull Lake -
74 Sacagawea Ridge - Cedar Ridge - Washakie Point]. [Hall and Jaworowski's \(1999\)](#) reevaluation of
75 the Cedar Ridge section showed that all of the Pleistocene allostratigraphic units ([NACSN, 1983](#))
76 above the Tertiary beds at Cedar Ridge should be correlated to Sacagawea Ridge-and-younger
77 deposits and are paleomagnetic-normal (no older than the Gauss-Matuyama boundary of 781 ka).
78 Thus, no evidence exists at this locality for Richmond's purported Cedar Ridge and Washakie Point
79 deposits. Likewise, recent ^{10}Be and ^{36}Cl exposure age-analyses from moraine boulders at the BLTA
80 ([Hall and Jaworowski, 1999](#); [Chadwick et al., 1997](#)) also found no evidence for pre-Sacagawea
81 Ridge units. Thus, since 1999, the oldest two of Richmond's three 'pre-Bull Lake' units are no
82 longer viable allostratigraphic units in the WRR, and that only the Sacagawea Ridge, Bull Lake, and
83 Pinedale remain as widely recognized units.

84 [Dahms \(2004a\)](#) used morphostratigraphy and soil development at Sinks Canyon to identify a
85 succession of allostratigraphic units (moraines) corresponding to the Pinedale (MIS2; [Cohen and](#)
86 [Gibbard, 2011](#)), Early Wisconsin (MIS4), Bull Lake (MIS6), Sacagawea Ridge (MIS16?) glaciations
87 as well as two stratigraphically older diamictons above/outside the canyon that suggested that
88 two older (undated) glacial advances were represented here. These were provisionally termed
89 Older and Younger pre-Sacagawea Ridge ([Dahms, 2004a](#)).

90 The previous model for the Lateglacial/Holocene (post-LGM) succession of the WRR ([Dahms et al.,](#)
91 [2010](#)) was based on cumulative relative and numeric age data gathered by numerous workers
92 from alpine valleys along the range ([Holmes and Moss, 1955](#); [Currey, 1974](#); [Dahms, 2002](#); [Gosse et](#)

93 al., 1995a, b, 1999; Mears, 1974; Miller and Birkeland, 1974; Mahaney, 1978, 1984a, b; Zielinski
94 and Davis, 1987). The main points of contention in this work have been (a) the age of those
95 deposits previously associated with the Younger Dryas (YD) and (b) the number and age(s) of
96 post-YD events preserved here. Early interpretations of the post-LGM succession focused chiefly
97 on the age of the type Temple Lake moraine in the Temple Lake Valley. Hack (1943) and Moss
98 (1949, 1951; Holmes and Moss, 1955) identified deposits corresponding to two late Pleistocene –
99 Holocene glacial advances here. Their work identified the Type Temple Lake moraine as a pre-
100 Altithermal unit and younger moraines corresponding to the ‘Little Glaciation’ (Little Ice Age).
101 Richmond (1965) later revised the interpretations of Holmes and Moss in the Temple Lake valley,
102 suggesting that two Temple Lake moraines were preserved here (“a” and “b”) that represented the
103 oldest two of three neoglacial (post-Altithermal) advances. Richmond also revised the name of the
104 Little Glaciation to Gannett Peak (Richmond, 1965; Benedict, 1968; Birkeland et al., 1971). Miller
105 and Birkeland (1974) later re-interpreted these deposits, using significant differences in moraine
106 and boulder weathering characteristics and soil development to suggest four YD-to-Holocene
107 glacial events are preserved here [Temple Lake, Early Neoglacial, Audubon equivalent (Benedict,
108 1973; Miller and Birkeland, 1974), Gannett Peak]. Most recently, Dahms (2002) and Dahms et al.
109 (2010) presented a revised post-LGM stratigraphy for the WRR that essentially mirrored
110 Birkeland and Miller’s correlations with suggested ages: Gannett Peak (LIA), Black Joe (1-2 ka),
111 Alice Lake (~5500-4000 yr), Temple Lake (YD-equivalent).

112 In this paper, we use a combination of new and recalculated ^{10}Be and ^{26}Al exposure ages from
113 successions of moraines, diamictons, and bedrock surfaces previously described by Dahms (2002,
114 2004a) and Fabel et al. (2004) from Table Mountain, Sinks Canyon-Stough Basin, and North Fork
115 Canyon-Cirque of the Towers to more tightly constrain the Pleistocene glacial succession for the
116 southern WRR (Fig. 2). As the WRR is the type locality for most of the Rocky Mountain glacial
117 sequence, an updated chronology here adds to a more complete understanding of the alpine
118 glacial succession in North America. Additionally, we present evidence for rates of ice retreat
119 along the Middle and North Forks of the PopoAgie (Po-po'-zhuh) Basin from the maximum
120 positions of Pinedale ice (MIS2) in Sinks and North Fork canyons at/near the Last Glacial
121 Maximum (LGM) to the Lateglacial positions of the cirque glaciers as represented by moraines in
122 Stough Basin and Cirque of the Towers.

123

124 **2. Study Area**

125 The Wind River Range (WRR) is located in the Middle Rocky Mountains of west-central Wyoming,
126 with the PopoAgie River basin on the range's southeastern flank (Fig. 1). Table Mountain, Sinks
127 Canyon and Stough Basin are parts of the Middle PopoAgie Basin while North Fork Canyon and the
128 Cirque of the Towers occupy most of the basin of the North Fork of the PopoAgie (Fig. 2). Table
129 Mountain and the mouth of Sinks Canyon are located ~15 km southwest of the city of Lander,
130 Wyoming. Sinks Canyon was the single outlet for the trunk glacier in the Middle PopoAgie Basin
131 and is the most southerly of the four major canyons along the eastern slope of the WRR (Fig. 1)
132 where Pleistocene glacial deposits previously were described (Richmond, 1957, 1986; Richmond
133 and Murphy, 1965, 1989; Murphy and Richmond, 1965; Shroba, 1989; Chadwick et al., 1997;
134 Phillips et al., 1997; Applegarth and Dahms, 2001; Dahms, 2004a). The mouth of North Fork
135 Canyon lies ~13 km northwest of Lander (Fig. 2). North Fork Canyon was the single outlet for the
136 North Fork Basin trunk glacier. Post-LGM glacial deposits were previously reported from Stough
137 Basin and Cirque of the Towers by Dahms and his colleagues (Dahms, 2002; Dahms et al., 2010).
138 Glacial deposits have not previously been described from the North Fork Canyon, downvalley from
139 Cirque of the Towers.

140 Bedrock of the areas sampled for this study is Archaean granite and granodiorite of the Louis Lake
141 Formation (Love and Christianson, 1985; Frost et al., 2000). Although Sinks and North Fork
142 canyons are carved into a nearly complete section of the Paleozoic limestones, dolomites, and
143 sandstones described for this region of Wyoming (Love et al., 1992), only granitic boulders and
144 bedrock exposures were sampled for this study.

145

146 **3. Materials and methods**

147 We combined recalculated ^{10}Be and ^{26}Al exposure age-data with newly-generated ^{10}Be ages to
148 obtain the best possible insight into the timing of the glacial advances and of the post-LGM ice
149 retreat in our study region. We acquired nineteen new samples from boulders on previously
150 identified moraines (Dahms, 2004a) associated with the Sinks Canyon trunk glacier (Pinedale, Bull
151 Lake, Sacagawea Ridge and pre-Sacagawea Ridge) and a previously unreported moraine at the

152 mouth of North Fork Canyon (Pine Bar Ranch). In the upper portion of Sinks Canyon, we re-
153 calculated eighteen ages from two previously-reported valley-side transects of polished-striated
154 bedrock (Fabel et al., 2004). We also present fifteen new ages from two cross-basin bedrock
155 transects in Stough Basin.

156 We report ten new ^{10}Be exposure ages from boulders on alpine moraines in Helen cirque (Stough
157 Basin) and in Cirque of the Towers that Dahms (2002; et al., 2010) previously correlated to the
158 Younger Dryas and 'Neoglacial' (Temple Lake and Alice Lake Alloformations). We include in our
159 interpretations fourteen recalculated ^{10}Be exposure ages previously developed by Marcott (2011)
160 from boulders on the Alice Lake-age and Temple Lake-age moraines in Bigfoot cirque (Fig. 6 in
161 Dahms et al., 2010) as well as eight boulders from the Type Temple Lake moraine in the Temple
162 Lake Valley (Marcott, 2011; locations S5a-S6b of Fig. 5C in Dahms et al., 2010). In order to
163 compare our interpretations with other regions in North America, we have recalculated surface
164 exposure-ages published prior to 2011.

165

166 3.1 ^{10}Be and ^{26}Al surface exposure ages

167 In order to obtain the most reliable exposure ages, we used commonly-accepted methods for
168 sampling moraine boulders (e.g., Gosse and Phillips, 2001; Masarik and Wieler, 2003). We chose
169 the largest available boulders with glacial polish and/or striations protruding more than 1m from
170 stable moraine ridges to avoid post-depositional tilting. We sampled boulders with relatively flat
171 tops to avoid edge effects. We also sampled exposures along two valley cross-sections in both
172 Sinks Canyon (Fabel et al., 2004) and Stough Basin that showed clear evidence of glacial polish
173 and/or striae.

174 The position (latitude/longitude and altitude) of each sample site was recorded with GPS and
175 verified with a topographic map as both have an influence on the amount of cosmic radiation. We
176 measured the dip of the boulder surface, the direction of the dip and the topographic shielding to
177 correct for the geometry of individual boulders and the effect(s) of topographic shielding by
178 surrounding mountains. We sampled only the uppermost 1-3 cm of boulders and 1-5 cm of the
179 bedrock transects and documented sample thickness to account for the attenuation of cosmic rays
180 with depth within the rock material.

181 For ^{10}Be analyses the rock samples were pre-treated following the procedures of [Kohl and](#)
182 [Nishiizumi \(1992\)](#) and [Ivy-Ochs \(1996\)](#). Samples were crushed and sieved and the quartz isolated
183 by treating the 0.25mm–0.6 mm fraction with *aqua regia* to destroy organic contaminations and
184 any calcareous components. After a 1h-treatment with 0.4% HF, we used a floatation system to
185 physically separate feldspar and mica components from quartz. Remnant feldspars and micas
186 were removed by repeated 4%HF leaching. Once pure quartz was obtained, we added a ^9Be -
187 carrier solution and dissolved the samples in 40%HF. Isotopic beryllium was isolated using anion
188 and cation exchange columns followed by selective pH precipitation techniques ([von](#)
189 [Blanckenburg et al., 1996](#)). The Be hydroxides were precipitated, dried, and calcinated to BeO at
190 850°C. The $^{10}\text{Be}/^9\text{Be}$ ratios were measured at two different accelerator mass spectrometry
191 facilities. New samples in Table 1 were analysed at the ETH Laboratory of Ion Beam Physics'
192 Accelerator Mass Spectrometry (AMS) facility using the ^{10}Be standard S2007N with a nominal
193 value of $^{10}\text{Be}/^9\text{Be} = 28.1 \times 10^{-12}$ ([Christl et al., 2013](#); [Kubik and Christl, 2010](#)). S2007N has been
194 calibrated to the ^{10}Be standard ICN 01-5-1 of K. Nishiizumi and has a nominal $^{10}\text{Be}/^9\text{Be}$ value of
195 2.709×10^{-11} ([Nishiizumi et al., 2007](#)). The 1σ error of S2007N is 2.7% ([Christl et al., 2013](#)). New
196 ^{10}Be and ^{26}Al data in Table 2 were determined at PRIME Lab, Purdue University between 1997 and
197 1999 and normalised to NIST SRM4325 with $^{10}\text{Be}/^9\text{Be} 2.68 \times 10^{-11}$, and Z92-0222 with $^{26}\text{Al}/^{27}\text{Al}$
198 4.11×10^{-11} . The original PRIME Lab $^{10}\text{Be}/^9\text{Be}$ results have been converted to be directly
199 comparable to the above $^{10}\text{Be}/^9\text{Be}$ standard value of 2.709×10^{-11} ([Nishiizumi et al., 2007](#)).
200 Measured $^{10}\text{Be}/^9\text{Be}$ ratios were corrected for ^{10}Be contributed by the Be-carrier determined from
201 process blanks ($^{10}\text{Be}/^9\text{Be}$ of 3.0×10^{-15} for both AMS laboratories). No correction was required for
202 $^{26}\text{Al}/^{27}\text{Al}$ measurements. Stable Al concentrations in aliquots of the dissolved quartz were
203 determined by flame atomic absorption spectrophotometry (AAS), using the method of standard
204 additions. Little to no matrix effect was observed, and [Al] measurements were reproducible to
205 2%. ^{10}Be and ^{26}Al AMS data and concentrations for the boulder and bedrock samples are reported
206 in Table S1 and S2, respectively.

207 All exposure ages reported here are calculated using CRONUS-Earth version 2.3
208 (<http://hess.ess.washington.edu/math/>) with the default production rates (4.01 ^{10}Be atoms/gram
209 SiO_2/year , 27.07 ^{26}Al atoms/gram SiO_2/year ; [Borchers et al., 2016](#)) and half-lives (^{10}Be half-life of
210 1.387 ± 0.012 Ma ([Chmeleff et al. 2010](#); [Korschinek et al., 2010](#)) and ^{26}Al half-life of 0.705 ± 0.018 Ma

211 (Nishiizumi 2004). The production rate was scaled for latitude, Longitude and altitude using the
212 time-dependent L_m scaling scheme (Lal, 1991; Stone, 2000). We corrected for sample thickness
213 assuming an exponential depth profile (Brown et al., 1992) with an effective radiation attenuation
214 length of 160 g cm^{-2} (Gosse and Phillips, 2001) and a rock density of 2.7 g cm^{-3} . Following Marcott
215 (2011) we assumed a rock erosion rate of 0 mm/ky for samples from those boulders ($\leq \text{LGM}$) that
216 exhibited glacial polish and striae. We used erosion rates of up to 2 mm/ky for boulders on older
217 Pleistocene deposits that exhibited progressively greater degrees of weathering with presumed
218 age according to their geomorphic relations. Although this method is rather subjective, these
219 relations appear to be useful. Note that the ages that we derive from boulders on Pinedale (0
220 mm/ky erosion rate) vs Bull Lake (2 mm/ky erosion rate) correspond well to ages of Pinedale and
221 Bull Lake moraines elsewhere in the WRR. We applied no correction for snow. Surface exposure
222 ages with one-sigma uncertainties for the boulder and bedrock samples are reported in Tables 1
223 and 2, respectively.

224

225 4. Results and Discussion

226 4.1 Table Mountain (Early Pleistocene)

227 Dahms (2004a) described the diamict on Table Mountain (Figs. 2, 3) and interpreted its age as
228 'pre-Sacagawea Ridge' (Early Pleistocene) on the basis of its geomorphic/stratigraphic position
229 and the soil weathering characteristics. ^{10}Be ages reported here from eight boulders at several
230 positions across Table Mountain range from >2000 to ca. 150 ka (Fig. 3, Table 1). The variability
231 of the exposure ages suggests two immediate interpretations: that (1) this material was deposited
232 in Early Pleistocene time and that (2) either many of the boulders were buried for much of their
233 histories and have more recently become exposed at the surface or those boulders with relatively
234 young exposure ages have undergone significant erosion since their deposition, or both.

235 The depths of original moraine matrix removed from above the once-buried boulders is unknown,
236 but it is apparently significant. Moraine erosion of $3\text{-}4 \text{ mm/ky}$ was needed to bring the ^{10}Be ages
237 of 1.5 m -diameter boulders at Dinwoody Lake, into concordance with the age of a 3 m -diameter
238 boulder, so that "... in 650 ka , an erosion rate of 0.35 cm ka (sic) would remove more than 2 m of
239 till from the crest" (Gosse et al., 2003). A similar calculation south of Dinwoody Lake on the Bull

240 Lake moraines at the BLTA suggested these moraine crests had lost more than 1.4 m of till in ~140
241 ka. Using these erosion estimates and our estimated ages of >1-2 Ma for the two oldest boulders,
242 it is possible that as much as 14 m of material has been removed from some portions of the Table
243 Mountain diamicton.

244 Boulder heights here do not appear to follow the common assumption that higher boulders exhibit
245 more dependable exposure ages (e.g., Gosse et al., 1995a). Heyman et al. (2016) show a generally
246 positive correlation between taller boulders and exposure age groups, but also note that a
247 dominant fraction of the groups still have scattered exposure ages. In this study, however, the two
248 oldest Table Mountain boulders (TM-1, 6) are less than three meters tall, while the tallest boulders
249 (ET-1, 2) exhibit comparably young ages. While Gosse et al. (2003) reported no relation between
250 boulder height and ¹⁰Be age on Bull Lake moraines at Fremont Lake (western slope WRR) they
251 reported a positive correlation on the Sacagawea Ridge moraine near Dinwoody Lake (eastern
252 slope). There are many possibilities for how boulders erode, either fast or slow, on any specific
253 landform, but the most obvious mechanism for boulder erosion over time at the present location
254 are fire and lightning strikes (Zimmerman et al., 1994; J.C. Gosse personal communication). The
255 high elevation of Table Mountain leaves it extremely exposed to thunderstorm activity and many
256 Lander-area residents have stories of lightning strikes and near-misses here during summer
257 afternoon horse-back rides.

258 The exposure ages (1-2 Ma) of the oldest two of the Table Mountain boulders (Fig. 3; TM-1, TM-6)
259 suggest that ice extended outside whatever form that Sinks Canyon took during the Early
260 Pleistocene and flowed over the position now occupied by the canyon of Sawmill Creek onto the
261 surface of Table Mountain (Dahms, 2004a; Züst et al., 2014). A re-entrant valley which now
262 separates the eastern from the western half of Table Mountain (Fig. 3) suggests that two separate
263 ice advances might be represented here. It appears that an older ice advance delivered material to
264 the eastern end of Table Mountain near the locations of samples ET-1 and ET-2 (Fig. 3). Additional
265 evidence for glacial ice at this location can be seen just north of boulder ET-2. A series of step-like
266 features here (Fig. 3 dashed orange lines) appear to be the remnants of kame terraces that mark
267 the southern margin of such an ice mass. The presence of two surfaces on separate sides of the re-
268 entrant suggests that either a recessional position of an older glacier or a separate (younger)

269 glacier terminated at the central portion of Table Mountain long enough for meltwater to remove
270 substantial amounts of the older material to form the re-entrant valley.

271 The position of the Table Mountain diamict over 400 m above the present Middle PopoAgie River
272 also suggests that, during the early Pleistocene, Sinks Canyon had not developed to the extent that
273 it's dimensions could contain all of the ice flowing from the basin's head. No erratic materials have
274 been found further outside Sinks Canyon to the north or south to suggest that ice occupied a route
275 different from the present position of the canyon. Similar boulder/diamict materials, however,
276 are found at similar elevations and positions outside/above the canyon mouths at other locations
277 along the eastern slope of the WRR (Veggian et al., 2010). Although no ages are currently available
278 for these deposits, we suggest the Table Mountain diamict represents a more extensive regional
279 pattern of glacial deposition during the early Pleistocene when few canyons had developed to
280 dimensions that would enable them to constrain the ice volume of their valley glaciers. This
281 situation appears to be analogous to Anderson et al's (2012) concept of 'far-flung moraines' where
282 older moraines often are found many kilometres beyond more recent moraines as an inevitable
283 consequence of glacial erosion over time wherever glacial erosion rates are greater than uplift
284 rates. Thus, the presence of these high elevation moraines/diamicts outside canyon mouths
285 suggests that we should revisit older models of 'pre-canyon' glacial events in this region of the
286 Rocky Mountains (Blackwelder, 1915; Richmond, 1948, 1957; Love, 1977; Mears, 1974; Veggian et
287 al., 2010).

288

289 4.2 Sacagawea Ridge (Early Middle Pleistocene)

290 The age of deposits associated with the Sacagawea Ridge glaciation in the WRR remains poorly
291 constrained (Gosse et al., 2003). Outwash terraces containing Lava Creek B tephra (~650 ka)
292 were earlier identified downstream from and/or correlated with Sacagawea Ridge moraines at
293 Dinwoody Lakes (Richmond and Murphy, 1965; Richmond, 1976). More recently, a new locality of
294 a previously identified Lava Creek B ash deposit has been identified in the gravels of the high
295 terrace at the Lander airport (Anders et al., 2009; Dahms and Egli, 2016; William McIntosh,
296 personal written communication, January 2018). However, few boulder exposure ages have been
297 reported from moraines correlated to the Sacagawea Ridge glaciation. Gosse et al. (2003) obtained

298 time-constant ^{10}Be exposure ages of 145-to-360 ka from four boulders on the Type Sacagawea
299 Ridge moraine at Dinwoody Lake. When erosion rate(s) were considered according to boulder
300 heights, the resulting boulder exposure ages were equivalent to ~ 650 ka. If a time-dependent
301 scaling were applied to this data, we estimate the ages would be >50 ka younger.

302 [Phillips et al. \(1997\)](#) developed ^{36}Cl exposure ages of ca. 261-to-99 ka from a suite of six boulders
303 on the Sacagawea Ridge moraine at the BLTA. No additional cosmogenic exposure ages have
304 been derived from moraines mapped as 'Sacagawea Ridge' prior to the current study ([Table 1](#) and
305 below).

306 A left lateral remnant moraine associated with an isolated field of erratic boulders is located south
307 and east of the mouth of Sinks Canyon ~ 220 meters below Table Mountain and ~ 150 meters
308 above the Middle PopoAgie River ([Fig. 3](#)). This material apparently represents a younger
309 glaciation than that represented by the diamict on Table Mountain. [Dahms \(2004a\)](#) interpreted
310 this material as 'Younger pre-Sacagawea Ridge' on the basis of its correspondence to the moraine
311 mapped on the south rim of Sinks Canyon (see location of DS-1 in [Figs 3 and 4](#)) and the moraine's
312 position relative to deposits within the canyon correlated to the Sacagawea Ridge Alloformation.
313 Erratic boulders scattered across the dip slope between the PopoAgie River and the lower slopes
314 Table Mountain (yellow dots on [Fig. 3](#)) are entirely constrained between the above remnant
315 moraine and the base of Table Mountain. No erratic or till material is located on the bedrock
316 dip slope between the moraine and the river ([Dahms, 2004a](#)). This pattern suggests the
317 'Sacagawea Ridge' glacier split into two ice streams at an outcrop of the Tensleep Sandstone just
318 above the Sinks. One ice stream flowed out over the canyon rim to the east across what is now
319 Sawmill Canyon to below the northwest end of Table Mountain ([Fig. 3](#)). This ice stream contained
320 boulder DS-1, which yields an exposure age of 556 ± 188 ka. The ice stream remaining in the
321 canyon continued down and out of the canyon, terminating ~ 3 km outside the canyon mouth. If
322 much of the Sacagawea Ridge glacier's volume remained constrained within the canyon, then
323 Sinks Canyon had enlarged enough by this time to constrain a larger ice volume than during the
324 earlier advance(s) (Table Mountain). If this unit is indeed Sacagawea Ridge-age, its geomorphic
325 position matches earlier interpretations from the BLTA and from Dinwoody Lakes that the
326 Sacagawea Ridge glaciation was the initial post-canyon event in the WRR ([Richmond, 1965, 1986](#)).

327 More evidence for the association of Sacagawea Ridge ice with the outlet of Sinks Canyon occurs
328 just outside the canyon's mouth. An area just north of the river contains a deposit of mixed
329 Sacagawea Ridge and Bull Lake-age materials that we interpret as stagnant ice debris
330 (moraine/outwash)(Fig. 3; Dahms, 2004a). Here Dahms (2004a) and Dahms et al. (2012)
331 described a deeply weathered soil profile (HR-1 in Fig. 3) with all granitic clasts completely
332 weathered to grus to a depth of over 2 meters. Bull Lake-age materials are admixed with the older
333 materials (HR-2 in Fig. 3; see below) as seen by their soil profiles that are less deeply weathered
334 with fewer, smaller clasts weathered to grus (Dahms, 2004a).

335 Thus, the evidence to support our interpretation that the deposits Dahms (2004a) earlier
336 correlated to a 'Younger pre-Sacagawea Ridge' glaciation are probably no younger than Sacagawea
337 Ridge includes the following:

- 338 (1) The associated materials lie above the Middle Popo Agie River between the higher (older)
339 deposits on Table Mountain and the lower (younger) Bull Lake deposits;
- 340 (2) the surface of the outwash terrace containing the Lava Creek ash at Lander airport (Anders
341 et al., 2009; Dahms and Egli, 2016; William McIntosh, personal written communication,
342 January 2018) grades to the lowest margin of the moraine/outwash described (above)
343 outside the canyon mouth;
- 344 (3) soil weathering characteristics suggest these are younger deposits than those described for
345 Table Mountain and older than those associated with Bull Lake-age deposits (Dahms, 2004a;
346 Dahms et al., 2012);
- 347 (4) our ~556 ka exposure age from boulder DS-1 (Figs. 3, 4; Table 1). This exposure age has a
348 relatively large uncertainty. With the 1 σ external uncertainty the age could be between 368
349 ka and 744 ka. Considering only internal error the uncertainty still places the age from 452
350 ka to 660 ka. Even with these uncertainties, the age certainly falls between that of the Table
351 Mountain diamict mapped above and the Bull Lake moraines mapped below and allows us to
352 make a reasonable assumption that this unit corresponds to the Sacagawea Ridge
353 Alloformation.

354

355 4.3 Bull Lake (Late Middle Pleistocene)

356 The Bull Lake glacial deposits mapped within Sinks Canyon are most obvious as a series of lateral
357 moraines along the ~6 km mid-portion of inner Sinks Canyon, from the Missouri Geology Camp to
358 PopoAgie Falls (Fig. 4). In this reach of the canyon they stand out above and beyond the inner-
359 most complex of Pinedale deposits on both sides of the canyon (Dahms, 2004a).

360 Our new ^{10}Be exposure ages for Bull Lake allostratigraphic units in Sinks Canyon (Dahms, 2004a)
361 are generally similar to those ages reported previously (using older production rates and scaling
362 models) by Chadwick et al. (1997) and Phillips et al. (1997) from the Bull Lake type Area (BLTA).
363 Boulders N-1, N-2 and N-3 on the moraine/outwash complex outside the mouth of Sinks Canyon
364 (Fig. 3; Table 1) yield exposure age-estimates between 93 ka and 163 ka. Additionally, we re-
365 calculated the ages from the two valley-side bedrock transects of Fabel et al. (2004), the upper
366 portions of which are associated with Bull Lake moraine units (Dahms, 2004a; Figs 3, 4; Table 1).
367 Our re-calculated ^{10}Be exposure-ages of ca. 130–to-69 ka (Table 2) support Fabel et al's (2004)
368 earlier interpretation that the bedrock between the Bull Lake and Pinedale map limits have been
369 more/less continuously exposed to cosmogenic radiation since the retreat of Bull Lake- or
370 possibly Early Wisconsin-age (MIS-4) ice from Sinks Canyon (Dahms, 2004a; Fabel et al., 2004;
371 Hall and Shroba, 1993, 1995; Colman and Pierce, 1986).

372

373 4.4 Pinedale (Late Pleistocene - LGM)

374 ^{10}Be exposure ages from two boulders on the terminal moraine at the mouth of North Fork
375 Canyon (Pine Bar Ranch, Fig. 2) indicate that the Pinedale glacier here abandoned its terminus ca.
376 22.5-23.3 ka (Table 1). From these ages, we estimate that the Pinedale glacier in Sinks Canyon (at
377 The Sinks; Fig. 4) reached its terminal position no later than ca. 22.5 ka. Our results are similar to
378 the mean exposure ages (as recalculated by Shakun et al., 2015) reported for LGM terminal
379 moraines from the Fremont Lake Type Area (FLTA; 23.2-22.5 ka), the Colorado Front Range
380 (Middle Boulder Creek, 20.6 ± 1.3 ka; Green Lake, 21.8 ± 2.4 ka; Clear Creek, 20.6 ± 0.5 ka; Pine Creek,
381 23.5 ± 1.5 ka), the Wallowa Mountains (24.2 ± 1.1 ka), the Uinta Mountains (E. Fork Smith's Fork
382 and S. Fork Ashley Creek (20.4 ± 2.4 ka, 22.5 ± 1.8 ka), the Ruby Mountains (22.7 ± 2.1 ka), and the
383 Sonora Junction moraines of the Sierra Nevadas (21.5 ± 0.8 - 22.5 ± 2.8 ka). We also note that Shakun

384 and Carlson (2010) have determined that the average global maximum ice extent was ca. 22 ka,
385 while Clark et al. (2009) place the duration of the LGM from 26.5 to 19.0 ka.

386

387 4.5 Lateglacial-to-Holocene

388 The period from ca. 19-11.5 ka is generally recognized as a period of global deglaciation (Shakun
389 et al., 2015). Moraines attributed to this period in the western United States generally are termed
390 as ‘recessional LGM’ deposits (Thackray, 2008) as the majority of exposure ages earlier than ~16
391 ka are reported from lateral and end moraines in the lower valleys of trunk glaciers (see Licciardi
392 et al., 2004; Munroe et al., 2006; Laabs et al., 2009; Leonard et al., 2017). ‘Lateglacial’ boulder
393 exposure ages associated with lower/outer cirque moraines from the western U.S. often are
394 correlated to the Younger Dryas (12.9-11.7 ka of Alley, 2000, Alley et al., 1993; also see Osborn et
395 al., 1995; Davis et al., 2009; Munroe and Laabs, 2017; Menounos and Reasoner, 1997; Osborn and
396 Gerloff, 1997).

397 A pattern of cold climate activity following the Heinrich-1 event (16.8 ka, Hemming, 2004) prior to
398 the Younger Dryas is already noted in regions of the U.S. west (Clark and Bartlein, 1995; Benson et
399 al., 1997) and exposure ages corresponding to cirque glacier activity at this time are common from
400 locales in the European Alps (Böhlert et al., 2011; Darnault et al., 2012; Ivy-Ochs, 2015; Palacios et
401 al., 2017; Makos et al., 2018). We are, however, aware of no previous accounts from the western
402 U.S. mountains where cirque moraines are explicitly attributed to glacial activity during the
403 ‘Oldest Dryas’ (17.5-14.7 ka; INTIMATE event GS-2.1a of Rasmussen et al., 2014). Mean boulder
404 exposure ages (Shakun et al., 2015) from the Junction Butte and Deckard flats (Yellowstone)
405 moraines (15.5±0.7, 15.8±1.3 ka;) and from the Outer and Inner Jenny Lake (Tetons) moraines
406 (15.9±0.9, 14.8±1.2 ka), however, suggest ice was active in these valleys at this time. Leonard et al.
407 (2017) also report 17-14 ka exposure ages from boulders on cirque and upper-valley moraines in
408 the Sangre de Cristo Mountains equivalent to the cirque/valley positions we report below. Thus,
409 while no correlations have been made from the western U.S. specifically to ‘Oldest Dryas’ glacial
410 activity, evidence begins to appear for this equivalence. In the following section we present
411 evidence for glacier activity during both the Younger and Oldest Dryas periods from three cirques
412 in the southern WRR.

413

414 4.5.1 Temple Lake Valley

415 We noted above that the Temple Lake Alloformation has previously been interpreted to
416 correspond to a glacial advance in the WRR during the Younger Dryas ([Hack,1943](#); [Moss, 1949,](#)
417 [1951](#); [Holmes and Moss, 1955](#); [Birkeland et al., 1971](#); [Miller and Birkeland, 1974](#); [Dahms, 2002, et](#)
418 [al., 2010](#)). Using the available data originally reported by [Marcott \(2011\)](#), we recalculated eight
419 exposure ages from boulders on the terminal moraine of the Temple Lake Type Locality here using
420 CRONUS 2.3 and the same time-dependent scaling (Lm) of Lal/Stone ([Lal, 1991](#); [Stone, 2000](#)). The
421 recalculated ages ([Table 1](#)) range from 12.4 ± 1.2 ka to 16.5 ± 1.6 ka [unweighted average (minus
422 young outlier) = 15.3 ± 1.5 ka]. This range of ages suggests the Type Temple Lake moraine most
423 likely was deposited during INTIMATE event GS-2.1a (17.5-14.7 ka; [Rasmussen et al., 2014](#);
424 [Shakun and Carlson, 2010](#); [Ivy-Ochs, 2015](#)), rather than during event GS-1 (Younger Dryas, 12.9-
425 11.7 ka; [Rasmussen et al., 2014](#); [Alley, 2000](#)).

426

427 4.5.2 Stough Basin & Cirque of The Towers

428 Discrete moraine units were previously identified both in Stough Basin and Cirque of the Towers.
429 through the use of relative age-characteristics. These units were correlated to four Lateglacial-
430 Holocene glacial advances ([Figs 5, 7](#); [Dahms, 2002](#); [Dahms et al., 2010](#)). The oldest/outer cirque
431 moraines ('Temple Lake') were correlated to the Younger Dryas (12.9-11.6 ka; [Alley, 2000](#)), while
432 the immediately younger/inner moraines ('Alice Lake') were associated with the first Neoglacial
433 advance of the Holocene (ca. 5-6 ka). The youngest two units were correlated to the Black Joe (1-2
434 ka) and Gannett Peak (LIA) alloformations. We present here new ^{10}Be exposure-ages from three
435 sets of Temple Lake and Alice Lake-age moraines in Stough Basin and Cirque of the Towers that
436 revise the previous correlations of these allostratigraphic units.

437 [Marcott \(2011\)](#) recently reported a series of ^{10}Be boulder exposure ages from the outer ('Temple
438 Lake') and middle ('Alice Lake') moraines in Bigfoot Lake cirque ([Fig. 5](#); [Table 1](#)). Our
439 recalculations of Marcott's fourteen exposure ages (CRONUS 2.3) show the outer ('Temple Lake')
440 moraine was deposited ca. 14.3 ± 1.4 ka while the middle ('Alice Lake') moraine was deposited ca.
441 11.0 ± 1.1 ka. These unweighted mean exposure ages are significantly older than Dahms' original

442 interpretations for these two moraines (Dahms, 2002; Fig. 6 in Dahms et al., 2010). Marcott,
443 however, recently detected (personal written communication, 2017) errors in his original data
444 table (Marcott, 2011: Table B2), particularly in the data for the middle moraine (Alice Lake).
445 Accounting for these errors, Marcott relates that the arithmetic mean of the corrected ages are
446 14.9 ka for the Bigfoot Lake outer moraine and 13.9 ka for the Bigfoot Lake inner moraine (pers.
447 written communication, 2017; Table 1).

448 In order to corroborate Marcott's revised ages for the Temple Lake and Alice Lake
449 allostratigraphic units in Stough Basin, we sampled additional boulders from moraines mapped as
450 'Temple Lake' and 'Alice Lake' in Helen Lake cirque, immediately southeast and adjacent to Bigfoot
451 Lake (Fig. 6 in Dahms et al., 2010). We obtained unweighted average exposure ages, respectively,
452 of 15.6 ± 1.6 ka ($n = 2$) and 13.2 ± 1.3 ka ($n = 2$) (Fig. 5; Table 1). These exposure ages largely agree
453 with Marcott's recalculated ages (above) from adjacent Bigfoot Lake cirque. When combined,
454 these age estimates indicate the moraines mapped as 'Temple Lake' and 'Alice Lake' in Stough
455 Basin were deposited ca. 15.6-14.9 ka and ca. 13.9-13.2 ka, respectively.

456 The relative age techniques used to differentiate the moraines in Stough Basin were also used to
457 distinguish the 'Temple Lake' from the 'Alice Lake' moraines in Cirque of the Towers (Fig. 4-F in
458 Dahms et al., 2010). Our six ^{10}Be exposure-ages from these moraines in Cirque of the Towers
459 closely correspond to the ages we report from Stough Basin.

460 The exposure ages of 11.2 ± 1.1 and 12.3 ± 1.3 ka from boulders CT-3 and CT-4 on the moraine
461 mapped as 'Alice Lake' (Fig. 4-F in Dahms et al., 2010; Fig. 8) are slightly younger than those we
462 report from the 'Alice Lake' moraines in Stough Basin (13.9-13.2 ka). Exposure ages from boulders
463 CT-1 and CT-2 of 15.8 ± 1.5 and 15.1 ± 1.5 ka (ave. = 15.5 ka; Table 1) on the moraine below
464 Warbonnet Peak mapped as 'Temple Lake' and the ages of boulders CT-5 and CT-6 of 15.1 ± 1.5 and
465 16.1 ± 1.6 (ave. = 15.6 ka) on the moraine enclosing Lonesome Lake (Fig. 8) indicate these
466 moraines most likely were formed synchronously. The most likely scenario is that the 'Temple
467 Lake' moraine below Warbonnet Peak is a right lateral moraine of the glacier that reached from
468 the southern cirque headwall down to Lonesome Lake. It is possible, however, that the moraine
469 enclosing Lonesome Lake was formed by ice flowing exclusively from the smaller cirques
470 surrounding Pingora Peak while the southern moraine is a terminal moraine formed by a separate
471 ice mass flowing from the Warbonnet Peak headwall (Fig. 8). The latter scenario would require

472 the receding North Fork trunk glacier to have separated above Lonesome Lake into two discrete
473 cirque glaciers prior to ~16.0 ka. The ice masses from the headwall above Pingora Peak would
474 then have re-advanced to the distal end of Lonesome Lake while the ice mass from the southern
475 cirque area advanced only far enough to deposit the southern 'Temple Lake' moraine. The mean
476 exposure age ($n = 4$) of 15.5 ± 1.5 ka from these two 'Temple Lake' moraines (Table 1; Figs 7, 8)
477 correspond closely to the mean ages we report from the 'Temple Lake' moraines in Stough Basin
478 [14.9 ka in Bigfoot cirque (Marcott, pers. written comm., 2017); 15.6 ka in Helen cirque](Figs 5, 8;
479 Table 1).

480 The general similarity of exposure ages from moraines correlated to the Alice Lake and Temple
481 Lake alloformations in Stough Basin and Cirque of the Towers indicates that these deposits were
482 formed by two advances of cirque glaciers during the Lateglacial period (post-LGM/pre-Holocene).
483 The similarity among the ^{10}Be exposure ages (Table 1; Fig. 9) from the 'Alice Lake' moraines in
484 Stough Basin (13.9-13.2 ka) and in Cirque of the Towers (11.8 ka) indicate that the Alice Lake
485 Alloformation in the southern Wind River Range most likely was formed during the extended
486 cooling period(s) of GI-1c3,2,1 through GS-1 [commonly termed the intra-Allerød cold period
487 (IACP)-Younger Dryas of 13.9-11.7 ka; Rasmussen et al., 2014; Alley, 2000; Shakun and Carlson,
488 2010; Yu and Eicher, 2001] and not during the Holocene 'Neoglacial' as earlier proposed by Dahms
489 (2002; Dahms et al., 2010). Additionally, the recalculated mean exposure age of 13.3 ± 0.6 ka for
490 the Titcomb Lakes moraine of the northern WRR (Gosse et al., 1995a, b; Shakun et al., 2015)
491 indicates this unit should also correspond to the Alice Lake Alloformation (as presently revised)
492 rather than to the Temple Lake Alloformation (Dahms et al., 2010).

493 We suggest that the means of the ages we report from the outer/older moraines in Stough Basin
494 ($n = 9$; ~15 ka) and Cirque of the Towers ($n = 4$; ~15.6 ka) closely correspond to the mean
495 exposure age of the boulders on the Type Temple Lake moraine ($n = 8$; ~15.3 ka) at the Temple
496 Lake Type Locality as recalculated from Marcott (2011). We propose that the Temple Lake
497 Alloformation in the southern Wind River Range should now correspond to the GS-2.1a event of
498 17.5-14.7 ka (commonly termed the Oldest Dryas; Rasmussen et al., 2014; Ivy-Ochs, 2015; Shakun
499 and Carlson, 2010) rather than to the Younger Dryas (Dahms et al., 2010 and references therein).

500

501 4.6 Post-LGM Recession

502 4.6.1 Sinks Canyon

503 Five new ^{10}Be ages on moraine boulders (Table 1) and eleven re-calculated ^{10}Be and ^{26}Al exposure
504 ages from polished/striated bedrock surfaces inside the highest-mapped Pinedale lateral
505 moraines (Table 2) constrain the rate at which the Sinks Canyon glacier receded 7.2 km from its
506 Pinedale terminal position at the Sinks. The arithmetic averages of boulder exposure ages from
507 end moraines Pd2 and Pd3 indicate the Pinedale glacier in Sinks Canyon had receded to 1.1 km
508 behind its estimated LGM position at The Sinks by 21.0 ka and to 2.6 km up-valley by ca. 19.4 ka
509 (Table 1; Fig. 4).

510 Two side-valley bedrock transects (Fig. 4; Fig. 5a and b; Fig. 5 in Fabel et al., 2004) located 5.5 km
511 and 7.2 km up-canyon from the Pinedale LGM position originally were used to demonstrate the
512 systematics of glacial erosion in bedrock-floored alpine valleys and to estimate rate(s) of bedrock
513 erosion. We re-calculated the ^{10}Be and ^{26}Al ages of Fabel et al. (2004) using updated scaling
514 estimates in order to identify when the basin floor at these localities became ice-free (Fig. 5; Table
515 2). The ^{10}Be exposure ages from the polished/striated bedrock surfaces along Transect B indicate
516 that the ice surface at the valley side-wall was near 2450 m at the LGM. By ~ 21.8 ka the ice
517 surface here had lowered to ~ 2420 m (#97-47/48). By ~ 19.0 ka the ice surface had lowered to
518 below ~ 2330 m (#97-85). The ^{10}Be exposure ages along Transect A-A' indicate the ice surface at
519 the valley-side was ice-free down to at least 2640 m (#97-113) by ~ 17.0 ka. ^{26}Al exposure ages
520 indicate that the ice surface had lowered to below 2560 m near the valley floor at the base of A-A'
521 by ~ 15.2 ka (#97-118, 120).

522 By using the two exposure ages of 22.5 ± 2.3 and 23.3 ± 2.3 ka from boulders on the Pinedale
523 terminal moraine at Pine Bar Ranch at the mouth of North Fork Canyon (Fig. 2; Table 1), we
524 estimate that the corresponding Pinedale glacier in Sinks Canyon had probably begun to recede
525 from its terminus by 22.5 ka. The average of the three boulder exposure ages from Sinks Canyon
526 moraine Pd2 (Fig. 4) indicates the glacier receded 1.1 km from its terminus to moraine Pd2 by
527 $21.0 \text{ ka} \pm 2.0$ at a rate between 0.31 and 1.1 m/yr. It receded up-valley another 1.5 km to Pd3 by
528 19.4 ± 1.8 ka at a rate of 1.1 to 1.2 m/yr. By the time the ice surface was below the base of Transect
529 A-A' at 15.3 ± 1.7 ka the glacier had receded another 4.6 km at a rate near 1.1 m/yr. We estimate

530 the glacier's overall recession rate from its terminus at the Sinks at 22.5 ka to 7.2 km up-canyon at
531 the base of transect A-A' at $\sim 15.3 \pm 1.7$ ka was from 0.7 to 1.3 m/yr.

532

533 4.6.2 North Fork Canyon

534 The two ^{10}Be exposure ages of 23.3 ± 2.3 and 22.5 ± 2.3 ka from boulders (PB-1, PB-2) on the
535 terminal moraine at the mouth of North Fork Canyon at Pine Bar Ranch (Fig. 2; Table 1) constrain
536 the age of the Pinedale maximum here to ca. 23.0 ± 2.3 ka. We derived two additional exposure ages
537 (Dickinson Park-1, Dickinson Park-2) from a small (~ 3 m-high) lateral moraine directly below
538 Dickinson Park near the juncture of the Dickinson Park & North Fork trails (Fig. 2). Using 22.5 ka
539 as the age for the onset of recession of the North Fork glacier from its Pinedale terminus, the
540 younger Dickinson Park exposure age (DP-2) suggests the North Fork glacier had receded 13.5 km
541 up-canyon by ca. 16.4 ± 1.6 ka; this suggests a recession rate of between 1.8 and 3.0 m/yr. If the age
542 estimate for boulder DP-2 is realistic, then this rate is $\sim 2x$ the recession rate we estimated for
543 Sinks Canyon (above). We assume that the age of ~ 26.9 ka for the second boulder is anomalous.
544 This small moraine lies near river-terrace level at the foot of a set of lateral moraines, so boulder
545 DP-1 may have originated from an older/higher moraine and lodged on the edge of this moraine
546 when the glacier's terminus probably was located less than ca. 0.1 km downvalley.

547 Further up-canyon, the range of exposure ages of the three boulders above Lizard Head Meadows
548 (Fig. 8) indicates that moraines from two separate glaciers are present at this locality. Our
549 sampling area was located at the confluence where the Bear Lake cirque valley meets the North
550 Fork valley (Fig. 8). Boulders CT-8 (14.8 ± 1.5 ka) and CT-9 (14.9 ± 1.5 ka) were located ~ 200 m
551 downvalley from boulder CT-7 (17.6 ± 1.7 ka). Boulders CT-8 and CT-9 thus appear to represent a
552 marginal moraine deposited by the Bear Lake cirque glacier that contacted the left lateral moraine
553 of the North Fork glacier after the North Fork glacier receded from this position. The ages of
554 boulders CT-8 and CT-9, thus, suggest this moraine is of late Temple Lake-age. Boulder CT-7,
555 therefore, represents a position of the North Fork trunk glacier as it receded up North Fork
556 Canyon into the Cirque of the Towers. This recessional sequence corresponds well with the 16.1 –
557 15.1 ka ages reported from boulders CT-5 and CT-6 on the moraine enclosing Lonesome Lake. If
558 boulder CT-7 represents a recessional position of the North Fork glacier at ~ 17.6 ka, then the

559 North Fork glacier receded 27 km up-canyon from its LGM position at Pine Bar Ranch at ~22.5 ka
560 to this position in Lizard Head Meadows at a rate of ~5.0 m/yr (5000 m/kyr). This recession rate
561 is 5x the rate we calculate for the Middle Fork (Sinks Canyon) glacier. In theory, valley glaciers
562 with smaller ice-shed areas should respond more quickly to changes in climate conditions than
563 those with larger areas (Davis et al., 2009). Thus, the higher recession rate of the North Fork
564 trunk glacier could be due to either its smaller ice-shed area (102 km²), when compared to that of
565 the Middle Fork trunk glacier (149 km²; Fig. 2) or differences in the hypsometry between the
566 basins (Young et al., 2011), as the Cirque of the Towers-North Fork basin is generally deeper than
567 Middle Fork basin.

568

569 4.6.3 Stough Basin

570 The Stough Basin valley trunk glacier at the LGM was composed of three coalescing cirque glaciers
571 from the Ice Lake, Bigfoot Lake and Helen Lake cirques (Figs. 2, 6). The glacier from Helen Lake
572 cirque occupied the eastern half of the basin; glaciers from Bigfoot Lake and Ice Lake cirques
573 occupied the middle and western areas, respectively. A medial moraine located near the basin's
574 center (Figs 6, 7a) apparently represents the location where the Helen Lake cirque glacier merged
575 with the glacier from Bigfoot Lake cirque to form most of the ice volume in Stough Basin. Riegels
576 at 3383 m and 3322 m impound the outer lakes in Helen and Bigfoot cirques, respectively.

577 With an area of 1.28 km², Helen cirque is the largest of the three cirques that fed ice to Stough
578 Basin; Bigfoot and Ice cirques are progressively smaller (0.83 and 0.19 km², respectively). As a
579 result, the Helen cirque ice stream most likely had the largest volume. We can estimate the upper
580 limit of the ice stream from the position of a remnant lateral moraine on the eastern valley wall
581 (see 97-90, 97-91 of Fig. 6). The upper elevation of this moraine remnant suggests that the
582 surface of the ice stream was no higher than ca. 3340 m at this location. The absence of erratic
583 boulders above the moraine suggests the Stough Basin ice surface may have reached no higher
584 than ca. 3360 m during either Pinedale or Bull Lake glaciations.

585 Exposure ages from the two erratic boulders (16.0±1.7 and 15.9±1.6 ka) on the lateral moraine
586 remnant (Fig. 6; Table 2), along with the 17.9±1.8 ka age of A-A' bedrock sample 97-68 (Fig. 7a)
587 suggest the ice surface in the basin still maintained much of its LGM elevation/thickness at ~18.0

588 ka, the same period the Middle Fork trunk glacier was retreating 6+ km from its terminus in Sinks
589 Canyon. The Stough Basin valley glacier apparently began to actively waste after ~18 ka (97-68).
590 Consequently, ice decay between 20 ka and 18 ka (#97-90, #91) was extremely fast at lower
591 elevations (cf. [Rigual-Hernández et al., 2016](#); [Monegato et al., 2017](#)) which finally translated to
592 high elevations after this time. [Note that lateral moraines generally form below ELA, so that the
593 moraine with samples 97-90 and 97-91 was probably near or below ELA by ~16.0 ka.] Ages from
594 the progressively lower bedrock surfaces along transects A and B ([Fig. 7a](#), 97-66, 97-63; [Fig. 7b](#),
595 97-97) indicate the surface elevation of the eastern ice stream emanating from Helen cirque
596 decreased by ca. 70 m, from 3350 -to- 3280 m, between 17.9 ka and 13.5 ka (ca. 20 m to 3330 m
597 by 14.8 ka and by another 50 m, to 3280 m, by 13.5 ka). Regardless of whether the true age of the
598 Temple Lake-age moraine in Helen cirque is closer to the youngest boulder exposure age
599 (13.9 ± 1.5 ka) or to the oldest ($\sim 17.2 \pm 1.7$ ka), the ages suggest that the ice immediately down-
600 valley from the riegel ([Fig. 7b](#), 97-97) lingered until sometime after ~14 ka. The ages of the
601 boulders on the Temple Lake-age moraine in Helen cirque indicate the moraine was deposited by
602 at least 13.9 ka. Thus, the ice in Helen cirque must have become detached across the riegels from
603 the valley glacier below before 16 ka for ice to have retreated behind the Helen Lake riegel far
604 enough to re-form the moraine. A similar situation is reported from the Uinta Mountains where
605 downwasting ice is suggested to have exposed higher cirque areas while active ice remained in the
606 lower valleys about this time ([Refsnider et al., 2008](#)).

607 On the west side of the basin the exposure age of 27.3 ± 2.9 ka from the highest, western-most
608 sample of transect A-A' (Figs. 6, 7; 97-100) indicates the elevation of the Pinedale maximum ice
609 surface in Ice Lake cirque was probably no higher than ca. 3460 m. The ~18.5 ka exposure age of
610 transect B-B' sample 97-75 indicates that as the ice surface here lowered following the LGM, ice
611 from Bigfoot cirque still extended over its northern wall and remained connected to the Ice Lake
612 ice stream. The mean of the bedrock exposure ages for 97-50, 97-52 and 97-55 ([Fig. 7a](#)) indicates
613 that by ~18.1 ka the Ice Lake ice surface had lowered below 3380 m. By ca. 17.0-16.5 ka the
614 surface of the ice flowing from Bigfoot cirque into Wilhelm Lake had lowered enough (from 3370
615 m to 3300 m) to expose the ridge separating Wilhelm Lake and Ice Lake ([Fig. 6](#); [Fig. 7b](#), 97-76; [Fig.](#)
616 [7a](#), 97-57, 59).

617 The exposure ages from samples 97-78 and 97-80 (Fig. 7b) suggest that ice had retreated from the
618 Bigfoot cirque riegel (~3330-3290 m) by at least 16.1 ka and possibly as early as 17.6 ka. Thus,
619 while the Helen Lake cirque glacier remained coupled to its down-valley ice stream until ~16-15
620 ka, ice in Bigfoot Lake cirque had already detached across the Bigfoot cirque riegel from the
621 remaining ice in the lower valley by 17-16 ka. Near the basin's center, the exposure age from 97-
622 62 (Figs. 6, 7a) indicates that stagnant ice remained on the floor of the basin east of Wilhelm Lake
623 until 12.5 ± 1.3 ka.

624 The decoupling of ice at the Bigfoot cirque riegel by 17-16 ka suggests that the ELA was not much
625 higher than ~3320 m (10,900') at this time -- a level that would allow relatively large areas of the
626 main valley glacier system (Deep Lakes, Ice Lakes) to remain above this elevation. It appears that
627 the surface of the Stough Basin ice stream quickly lowered and stagnated following the LGM while
628 the Middle Fork trunk glacier remained active with ice from the Deep and Ice lakes systems,
629 although in negative mass balance. This relationship supports the observation that the Stough
630 Basin glacier was no more than a secondary source of ice to the Middle Fork-Sinks Canyon trunk
631 glacier (and probably stopped contributing ice to the Middle Popo Agie trunk glacier about this
632 time), while the main accumulation areas were located in the Deep Creek Lakes/Ice Lakes cirque
633 valleys to the northwest (Fig. 2).

634 The Bigfoot and Helen cirque riegels are ca. 18.8 km upvalley from the Pinedale glacier's LGM
635 terminus at the Sinks. Our exposure ages indicate that the terminus of the PopoAgie trunk glacier
636 still extended to near transect A-A' (Fig. 5a) at ~15.3 ka in Sinks Canyon, while the ice surface in
637 Stough Basin had already lowered enough to expose the Bigfoot cirque riegel by ~17 ka. Thus,
638 while the Middle Fork glacier in Sinks Canyon receded relatively slowly from its terminus to
639 transect A-A' (0.7-1.3 m/yr), the overall rate of down-wasting, as calculated from the estimated
640 age when ice began to recede from the Pinedale terminus at 22.5 ka to the time ice abandoned the
641 Helen and Bigfoot cirque riegels (≥ 16 ka) is 2.9 m/yr.

642

643 5. Conclusions

644 5.1 Sinks Canyon – Table Mountain

645 Our ^{10}Be and ^{26}Al exposure ages from moraine boulders and polished/striated bedrock from the
646 Middle Fork and North Fork basins of the PopoAgie River more tightly constrain the sequence of
647 Pleistocene glacial activity previously reported for the PopoAgie Basin (Dahms, 2002, 2004a;
648 Dahms et al., 2010). Exposure ages from moraine boulders on alloformations in/near Sinks
649 Canyon correspond to at least four periods of glacial activity during the Early, Middle, and Late
650 Pleistocene. The oldest boulder exposure ages of 1.0-2.0 Ma from the Table Mountain diamict
651 previously identified as an undated Older pre-Sacagawea Ridge deposit (Dahms, 2004a) now
652 likely relates this diamict to an episode of Early Pleistocene pre-canyon glacial activity. We
653 propose the Table Mountain diamict should be identified as the Table Mountain Alloformation
654 and associated with at least one Early Pleistocene pre-canyon glaciation.

655 The single boulder exposure age of ca. 556 ka, when combined with the geomorphic
656 characteristics of the corresponding patches of isolated boulders and diamicts extending from
657 below Table Mountain onto and along the south rim of Sinks Canyon (Figs 2, 3) tentatively
658 suggests that Dahms' (2004a) original 'Younger pre-Sacagawea Ridge' unit now corresponds more
659 closely to the Sacagawea Ridge Alloformation. When combined with previous studies from the
660 eastern WRR that describe outwash terraces containing Lava Creek B tephra (~650 ka) that grade
661 to the Sacagawea Ridge moraines at Dinwoody Lakes and near the BLTA (Richmond and Murphy,
662 1965; Richmond, 1976; Chadwick et al., 1997), our boulder exposure age and new Lava Creek ash
663 locality at the Lander airport terrace (Dahms and Egli, 2016; William McIntosh, personal written
664 communication, January 2018) indicate this diamict more than likely corresponds to the
665 Sacagawea Ridge Alloformation and is most likely of MIS-16 age (Cohen and Gibbard, 2011).
666 However, in light of its large external uncertainty, taken by itself our ^{10}Be exposure age could
667 represent a span of MIS stages from 10 to 18.

668 Exposure ages from boulders on the moraines at the mouth of North Fork Canyon (Fig. 2) indicate
669 the Pinedale valley glacier advanced to the present location of the Pine Bar Ranch by ca. 23 ka.
670 This age closely corresponds to the recalculated ages (Shakun et al., 2015) of ~20-23 ka from the
671 oldest distal LGM moraines at the Fremont Lake Type Area (Wyoming), the Colorado Front Range,
672 the Sierra Nevadas and ages from the Uinta Mountains (Munroe and Laabs, 2017) -- all of which
673 generally correspond to Shakun and Carlson's (2010) estimate of 22-23 ka for the global LGM.

674 Boulder exposure ages from moraines outside and within Sinks Canyon (Table 1; Fig. 4) and re-
675 calculated ages from polished-striated bedrock along two valley-side transects (Fig. 4; Table 2;
676 Fabel et al., 2004) corroborate their previous associations with the Bull Lake and Pinedale
677 alloformations (Dahms, 2004a) and with MIS-6/5 and MIS-2, respectively. We were unable to find
678 datable boulders from moraines previously mapped by Dahms (2004a) as Early Wisconsin (MIS4)
679 and so the presence here and the age of this alloformation remains uncertain.

680

681 5.2 Stough Basin and Cirque of the Towers

682 Relations among the exposure ages from the two boulders on the lateral moraines on the east wall
683 of Stough Basin (Tables 1 and 2; Fig. 6), the bedrock ridge between Ice and Wilhelm lakes and the
684 moraines in Helen and Bigfoot cirques suggest the ice streams emanating from them began to
685 stagnate after ~18 ka. Stagnant ice probably remained on the southern floor of Stough Basin until
686 ~14-12 ka, but active cirque ice had decoupled across the cirque riegels and retreated behind the
687 cirque riegels by 17-16 ka. In a similar manner, exposure ages on the moraine boulders in Lizard
688 Head Meadows suggest that the North Fork trunk glacier retreated far enough into Cirque of the
689 Towers after 17 ka for it to have re-advanced to form the Lonesome Lake moraines by ~15.6 ka.

690 Boulder exposure ages from Stough Basin and Cirque of the Towers (Table 1; Fig. 9) show that the
691 outer-most cirque moraines in the southern WRR were formed during the Lateglacial Pleistocene
692 rather than the Holocene. The exposure ages from Bigfoot, Helen, Cirque of the Towers and the
693 Temple Lake Type Locality indicate that the Temple Lake Alloformation in the WRR now should
694 be considered coeval with the INTIMATE GS-2.1a cooling event of 17.4-14.7 ka commonly known
695 as the Older Dryas (Rasmussen et al., 2014; Benson et al., 1997; Shakun and Carlson, 2010; Ivy-
696 Ochs, 2015) rather than with the Younger Dryas, as earlier interpreted by Dahms (2002; Dahms et
697 al., 2010 and references therein). Following a recession, presumably during the Bølling-Allerød
698 interstadial, these cirque glaciers re-advanced in response to the IACP-Younger Dryas stadial(s) to
699 form moraines of the Alice Lake Alloformation. Thus, we revise Dahms' earlier correlation of the
700 Alice Lake alloformation with the mid-Holocene 'Neoglacial' period (2002; et al., 2010) and
701 propose that the deposits corresponding to the Alice Lake Alloformation in Stough Basin and
702 Cirque of the Towers are most likely coeval with the extended IACP-Younger Dryas cooling

703 episode (Fig. 9) and it is possible that evidence no longer exists for early- to mid-Holocene glacial
704 events in the southern Wind River Range.

705 The above suggested equivalences to the Oldest Dryas and Younger Dryas Lateglacial stadial
706 events are supported by the $\delta^{18}\text{O}$ data derived from the GISP2 and NGRIP ice cores (Stuiver et al.,
707 1995; Grootes and Stuiver, 1997; Rasmussen et al., 2014), the Owens Lake sediment cores
708 (Benson et al., 1997). Cirque moraines reported to result from glacial activity during the Younger
709 Dryas are common from the western U.S. (Osborn et al., 1995; Davis et al., 2009). Explicit reports
710 of cirque moraines attributed to activity during the Older Dryas period are few in the western U.S.
711 (although recalculations of previous exposure ages suggest equivalents may exist) while reports of
712 moraines corresponding both to the Egesen (Younger Dryas equivalent) and Gschnitz (Older
713 Dryas equivalent) advances of the European Alps are common (e.g., Darnault et al., 2012; Böhlert
714 et al., 2011; Ivy-Ochs, 2015; Palacios et al., 2017; Makos et al., 2018).

715 In order to refine and test the ideas presented here and place them within a coherent record of
716 landscape evolution, future work in this region should focus on:

- 717 (1) Identification of new exposures of early Pleistocene deposits. The geomorphic expression
718 of the Table Mountain diamicton suggests that more than one allostratigraphic unit may be
719 represented here. Additional paleomagnetic and numeric age-analyses should be applied to
720 isolated high-elevation landforms in situations similar to Table Mountain outside the
721 canyon mouths (e.g., Veggian et al., 2010);
- 722 (2) More accurate exposure ages for the Sacagawea Ridge allostratigraphic unit. The presently
723 available evidence makes it possible to place this unit anywhere from MIS-10 to MIS-18;
- 724 (3) Additional exposure ages from moraines and bedrock in the Deep Lakes and Ice Lakes
725 basins in order to estimate the recession rate of the Middle Popo Agie trunk glacier;
- 726 (4) Additional western U.S. localities for the rate(s) of recession of valley glaciers from their
727 terminal LGM position(s).
- 728 (5) Additional exposure age-estimates from the Type Alice Lake moraine of the southern Wind
729 River Range;
- 730 (6) Additional well-dated evidence of the geomorphic and stratigraphic record of all post-LGM
731 advances in the region, how well these records represent a global record of deposits
732 formed in response to Lateglacial stadial and inter-stadial climate cycles (e.g., Heinrich

733 events; the Blytt-Sernander sequence), the Holocene record of climate cycling (the 8.2 ka
734 event; the 'Neoglacial') and regional-to-global rhythms of climate change (e.g., [Clark and](#)
735 [Bartlein, 1995](#); [Yu and Eicher, 1998, 2001](#); [Shakun and Carlson, 2010](#); [Ivy-Ochs, 2015](#)).
736 (7) ELA reconstructions and glacial modelling, in order to further test some of our proposed
737 correlations and deglaciation geometries.

738

739 **Acknowledgments**

740 Exposure ages for the valley transects were funded by NSF grant SBR-9631437 to Fabel and
741 Harbor. The TM1-6 boulder exposure ages were funded by a Purdue University PRIME Lab seed
742 grant to Dahms. The project was also supported by a number of UNI Graduate College Summer
743 Fellowships. Sampling within the Washakie District of Shoshone National Forest was performed
744 under Special Use Permit #2037-01. We thank Jack and Alice Nicholas and the Raynolds family of
745 Lander, Wyoming and the staffs of Sinks Canyon State Park and the Diamond-4 Ranch for access to
746 sampling areas. We thank our reviewers for providing professional, insightful and, most
747 importantly, useful reviews by which we were able to significantly improve the manuscript.

748

749 **References**

- 750 Alley, R.B., Meese, D.A., Shuman, C.A., Gow, A.J., Taylor, K.C., Grootes, P.M., White, J.W.C., Ram, M.,
751 Waddington, E.D., Mayewski, P.A. and Zielinski, G.A., 1993. Abrupt increase in Greenland snow
752 accumulation at the end of the Younger Dryas Event. *Nature* 362: 527-529.
- 753 Alley, R.B., 2000. The Younger Dryas cold interval as viewed from central Greenland. *Quat. Sci. Rev.* 19,
754 213-226.
- 755 Anders, M.H., Saltzman, J., Hemming, S.R., 2009. Neogene tephra correlations in eastern Idaho and
756 Wyoming: Implications for Yellowstone hotspot-related volcanism and tectonic activity. *Geol. Soc. Am.*
757 *Bull.* 121, 827-856.
- 758 Anderson, R.S., Dühnforth, M., Colgan, W., Anderson, L. 2012. Far-flung moraines: Exploring the feedback of
759 glacial erosion on the evolution of glacier length. *Geomorphology* 179, 269-285.
760 [dx.doi.org/10.1016/j.geomorph.2012.08.018](https://doi.org/10.1016/j.geomorph.2012.08.018)
- 761 Applegarth, Michael T. and Dahms, Dennis E., 2001. Soil catenas of calcareous tills, Whiskey Basin,
762 Wyoming, USA. *Catena* 42, 17-38.
- 763 Benedict, J.B., 1968. Recent glacial history of an alpine area in the Colorado Front Range, U.S.A., II: Dating
764 the glacial deposits. *J. of Glac.* 7, 77-87.

- 765 Benedict, J.B., 1973. Chronology of Cirque Glaciation, Colorado Front Range. *Quat. Res.* 3, 584-599.
- 766 Benson, L., Burdett, J. Lund, S. Kashgarian, M., Mensing, S., 1997. Nearly synchronous climate change in the
767 Northern Hemisphere during the last glacial termination. *Nature* 388, 263-265.
- 768 Birkeland, P.W., Crandell, D.R. and Richmond, G.M., 1971. Status of correlation of Quaternary stratigraphic
769 units in the western conterminous United States. *Quat. Res.* 1, 208-227.
- 770 Blackwelder, E., 1915. Post-Cretaceous history of the mountains of western Wyoming. *J. Geol.* 23, 302-340.
- 771 Böhlert, R., Egli, M., Maisch, M., Brandova, B., Ivy-Ochs, S., 2011. Application of a combination of dating
772 techniques to reconstruct the Lateglacial and early Holocene landscape history of the Albula region
773 (eastern Switzerland). *Geomorphology* 127, 1-13.
- 774 Borchers, B., Marrero, S., Balco, G., Caffee, M., Goehring, B., Lifton, N., Nishiizumi, K., Phillips, F., Schaefer, J.,
775 Stone, J., 2016. Geological calibration of spallation production rates in the CRONUS-Earth project. *Quat.*
776 *Geochron.* 31, 188-198. [dx.doi.org/10.1016/j.quageo.2015.01.009](https://doi.org/10.1016/j.quageo.2015.01.009)
- 777 Brown, E.T., Edmond, J.M., Raisbeck, G.M., Yiou, F., Desgarceaux, S., 1992. Effective attenuation length of
778 cosmic rays producing ^{10}Be and ^{26}Al in quartz: implications for surface exposure dating. *Geophys. Res.*
779 *Lett.* 9, 369-372.
- 780 Chadwick, O.A., Hall, R.D., Phillips, F.M., 1997. Chronology of Pleistocene glacial advances in the central
781 Rocky Mountains. *Geol. Soc. Am. Bull.* 109, 1443-1452.
- 782 Chmeleff, J., von Blanckenburg, F., Kossert, K., Jakob, D., 2010. Determination of the ^{10}Be half-life by
783 multicollector ICP-MS and liquid scintillation counting. *Nucl. Insts. Meths. Phys. B* 268, 192-199.
- 784 Christl, M., Vockenhuber, P.W., Kubik, P.W., Wacker, L., Lachner, J., Alfimov, V., Synal, H.-A., 2013. The ETH
785 Zurich AMS facilities: Performance parameters and reference materials. *Nucl. Insts. Meths. Phys. B* 294,
786 29-38.
- 787 Clark, P.U. and Bartlein, P.J., 1995. Correlation of Late Pleistocene glaciation in the western United States
788 with North Atlantic Heinrich events. *Geology* 23, 483-486.
- 789 Clark, P.U., Dyke, A.S., Shakun, J.D., Carlson, A.E., Clark, J., Wohlfarth, B., Mitrovica, J.X., Hostetler, S.W., McCabe,
790 A.M., 2009. The Last Glacial Maximum. *Science* 325, 710-714.
- 791 Cohen, K.M., Gibbard, P., 2011. Global chronostratigraphical correlation table for the last 2.7 million years.
792 Subcommission on Quaternary Stratigraphy (International Commission on Stratigraphy), Cambridge,
793 England.
- 794 Colman, S. M., and Pierce, K. L., 1986. Glacial sequence near McCall, Idaho: weathering rinds, soil
795 development, morphology, and other relative age criteria. *Quat. Res.* 25, 25-42.
- 796 Currey, D.L., 1974. Probable pre-Neoglacial age for the type Temple Lake moraine, Wyoming. *Arct. Alp. Res.*
797 6, 293-300.
- 798 Dahms, D.E., 2002. Glacial Stratigraphy of Stough Creek Basin, Wind River Range, Wyoming.
799 *Geomorphology* 42, 59-83.
- 800 Dahms, D.E., 2004a. Relative and numeric age data for Pleistocene glacial deposits and diamictons in and
801 near Sinks Canyon, Wind River Range, Wyoming, U.S.A. *Arct. Alp. Res.* 36, 59-77.

- 802 Dahms, D.E., 2004b. Glacial limits in the Middle and Southern Rocky Mountains, USA, south of the
803 Yellowstone Ice Cap. In, Ehlers, J., Gibbard, P.L. (Eds.), Quaternary Glaciations – Extent & Chronology,
804 Part II: North America. Develops. in Quat. Sci., Vol 2b, Elsevier, Amsterdam, 269-282.
- 805 Dahms, D.E. and Egli, M., 2016. Carbonate and elemental accumulation rates in arid soils of mid-to-late
806 Pleistocene outwash terraces, southeastern Wind River Range, Wyoming, USA. *Chem. Geol.* 446, 147-
807 162. [dx.doi.org/10.1016/j.chemgeo.2015.12.006](https://doi.org/10.1016/j.chemgeo.2015.12.006)
- 808 Dahms, D.E., Birkeland, P.W., Shroba, R.R., Miller, C. Dan, Kihl, R., 2010. Latest Quaternary Glacial and
809 Periglacial Stratigraphy, Wind River Range, Wyoming. *Geol. Soc. Am., Digital Maps and Charts Series #7*,
810 46 p., doi: 10.1130/2010.DMCH007.
- 811 Dahms, D., Favilli, R. Krebs, M. Egli., 2012. Soil weathering and accumulation rates of oxylate-extractable
812 phases derived from alpine chronosequences of up to 1Ma in age. *Geomorph.* 151-152: 99-113,
813 doi:10.1016/j.geomorph.2012.01.021.
- 814 Darnault, R., Rolland, Y., Braucher, R., Bourlès, D., Revel, M., Sanchez, G., 2012. Timing of the last
815 deglaciation revealed by receding glaciers at the Alpine-scale: impact on mountain geomorphology.
816 *Quat. Sci. Rev.* 31, 127-142.
- 817 Davis, P. Thompson; Menounos, Brian; Osborn, Gerald, 2009. Holocene and latest Pleistocene alpine glacier
818 fluctuations: a global perspective. *Quat. Sci. Rev.* 28, 2021-2033.
- 819 Fabel, D., Harbor, J., Dahms, D., James, A., Elmore, D., Horn, L., Daley, K., Steele, C., 2004. Spatial patterns of
820 glacial Erosion at a valley scale derived from terrestrial cosmogenic ^{10}Be and ^{26}Al concentrations in
821 rock. *Ann. Assoc. Am. Geogr.* 94, 241–255.
- 822 Frost, B. R., Frost, C. D., Hulsebosch, T. P., and Swapp, S. M., 2000. Origin of the charnockites of the Louis
823 Lake batholith, Wind River Range, Wyoming. *Journal of Petrology*, 41: 1759–1776. Gosse, J.C., Evenson,
824 E.D., Klein, J., Lawn, B. and Middleton, R., 1995a. Precise cosmogenic ^{10}Be measurements in western
825 North America: Support for a global Younger Dryas cooling event. *Geology* 23, 877-80.
- 826 Gosse, J.C., Phillips, F.M., 2001. Terrestrial in situ cosmogenic nuclides: theory and application. *Quat. Sci.*
827 *Rev.* 20, 1475-1560.
- 828 Gosse, J.C., Evenson, E.D., Klein, J., Lawn, B., Middleton, R., 1995a. Precise cosmogenic ^{10}Be measurements
829 in western North America: Support for a global Younger Dryas cooling event. *Geology* 23, 877-880.
- 830 Gosse, J.C., Klein, J., Evenson, E.B., Lawn, B. and Middleton, R., 1995b. Beryllium-10 dating of the duration
831 and retreat of the last Pinedale glacial sequence. *Science* 268, 1329-1333.
- 832 Gosse, J., Davis, P.T., Burr, G., Jull, T., Bozarth, S., Sorenson, C., Klein, J., Lawn, B., Dahms, D., 1999. Late
833 Pleistocene/Holocene glacial and paleoclimatic history of Titcomb Basin, Wind River Range, Wyoming
834 based on lake sediments and cosmogenic nuclide dating. *Geol. Soc. Am. Abs. Programs* 31, 7, A-56.
- 835 Gosse, J.C., Evenson, E.B., Klein, J., Sorenson, C.J., 2003. Cosmogenic nuclide glacial geochronology in the
836 Wind River Range, Wyoming. In, Easterbrook, D. (Ed.), *Quaternary Geology of the United States*,
837 INQUA 2003 Field Guide Vol, p. 49-56. Desert Research Institute, Reno, Nv.
- 838 Grootes, P.M., and M. Stuiver. 1997. Oxygen $^{18}/^{16}$ variability in Greenland snow and ice with 10^3 to 10^5 -
839 year time resolution. *J. Geophys. Res.* 102, 26455-26470.

- 840 Hack, J.T., 1943. Antiquity of the Finley site. *Am. Antiq.* 8, 235-241.
- 841 Heyman, J., Applegate, P.J., Blomdin, R., Gribenski, N., Harbor, J.m., Stroeven, A., 2016. Boulder height –
842 exposure age relationships from a global glacial ^{10}Be compilation. *Quat. Geochron.* 34, 1-11.
843 [dx.doi.org/10.1016/j.quatgeo.2016.03.002](https://doi.org/10.1016/j.quatgeo.2016.03.002)
- 844 Holmes, G.W. and Moss, J.H., 1955. Pleistocene geology of the southwestern Wind River Mountains,
845 Wyoming. *Geol. Soc. Am. Bull.* 66, 629-653.
- 846 Hall, R.D., Jaworowski, C., 1999. Reinterpretation of the Cedar Ridge section, Wind River Range, Wyoming:
847 Implications for the glacial chronology of the Rocky Mountains. *Geol. Soc. Am. Bull.* 111, 1233-1249.
- 848 Hall, R. D., and Shroba, R. R., 1993. Soils developed in the glacial deposits of the type areas of the Pinedale
849 and Bull Lake glaciations, Wind River Range, Wyoming, U.S.A. *Arct. Alp. Res.* 25, 368–373.
- 850 Hall, R. D., and Shroba, R. R., 1995. Soil evidence for a glaciation intermediate between the Bull Lake and
851 Pinedale glaciations at Fremont Lake, Wind River Range, Wyoming, USA. *Arct. Alp. Res.* 27, 89–98.
- 852 Hemming, S. R., 2004. Heinrich events: Massive late Pleistocene detritus layers of the North Atlantic and
853 their global climate imprint, *Rev. Geophys.* 42, RG1005, doi:10.1029/2003RG000128.
- 854 Holmes, G.W. and Moss, J.H., 1955. Pleistocene geology of the southwestern Wind River Mountains,
855 Wyoming. *Geol. Soc. Am. Bull.* 66, 629-654.
- 856 Ivy-Ochs S. 1996. The dating of rock surfaces using in situ produced ^{10}Be , ^{26}Al and ^{36}Cl , with examples
857 from Antarctica and the Swiss Alps. PhD dissertation No. 11763, ETH Zürich.
- 858 Ivy-Ochs, S. 2015. Glacier variations in the European Alps at the end of the last glaciation. *Cuad. de Invest.*
859 *Geog.* 41(2), 295-315. doi: 10.18172/cig.2750
- 860 Kohl, C.P., Nishiizumi, K., 1992. Chemical isolation of quartz for measurement of in-situ produced
861 cosmogenic nuclides. *Geochim. Cosmochim. Acta* 56, 3583-3587.
- 862 Kubik, P.W., Christl, M., 2010. ^{10}Be and ^{26}Al measurements at the Zurich 6 MV Tandem AMS facility. *Nuc.*
863 *Instr. Meth B* 268, 880-883.
- 864 Korschinek, G., Bergmaier, A., Faestermann, T., Gerstmann, U., Knie, K., Rugel, G., Wallner, A., Dillmann, I.,
865 Dollinger, G., Von Gostomski, C.L., et al., 2010. A new value for the half-life of ^{10}Be by heavy-ion elastic
866 recoil detection and liquid scintillation counting. *Nucl. Instrum. Methods Phys. Res. Sect. B Beam Interact.*
867 *Mater. Atoms* 268, 187e191.
- 868 Laabs, B.J.C., Refsnider, K.A., Munroe, J.S., Mickelson, D.M., Applegate, P.J., Singer, B.S., Caffee, M.W., 2009.
869 Latest Pleistocene glacial chronology of the Uinta Mountains: support for moisture-driven asynchrony of
870 the last deglaciation. *Quat. Sci. Rev.* 28, 1171-1187. doi:10.1016/j.quascirev.2008.12.012
- 871 Lal, D., 1991. Cosmic ray labeling of erosion surfaces: in situ nuclide production rates and erosion models.
872 *Earth Planet. Sci. Lett.* 104, 424e439.
- 873 Leonard, E., Laabs, B.J.C., Plummer, M., Kroner, R., Brugger, K., Spiess, V., Refsnider, K., Xia, Y., Caffee, M.,
874 2017. Late Pleistocene glaciation and deglaciation in the Crestone Peaks area, Colorado Sangre de
875 Cristo Mountains, USA – Chronology and paleoclimate. *Quat. Sci. Rev.* 158, 127-144.

- 876 Licciardi, J.M. & Pierce, K.L., 2008. Cosmogenic exposure-age chronologies of Pinedale and Bull Lake
877 glaciations in greater Yellowstone and the Teton Range, USA. *Quat. Sci. Rev.* 27, 814-831.
- 878 Licciardi, J.M., Clark, P.U., Brook E.J., Elmore, D., Sharma, P., 2004. Variable responses of western US glaciers
879 during the last deglaciation. *Geology* 32, 81-84.
- 880 Locke, W., 1990. Late Pleistocene glaciers and the climate of western Montana, U.S.A. *Arct. Alp. Res.* 22, 1-
881 22.
- 882 Locke, W. and Smith, L.N., 2004. Pleistocene mountain glaciation in Montana, USA. *In: Ehlers, J., Gibbard,*
883 *P.L. (Eds.), Quaternary Glaciations – Extent & Chronology, Part II: North America. Dev. Quat. Sci. 2b,*
884 *125-129. Elsevier, Amsterdam.*
- 885 Love, J.D. 1977. Summary of Upper Cretaceous and Cenozoic stratigraphy, and the tectonic and glacial
886 events in Jackson Hole, Northwestern Wyoming. *Wyo. Geol. Assoc. Guidebook, 29th Ann. Field Conf.,*
887 *585-593.*
- 888 Love, J.D. and Christianson, A.C., 1985. Geologic map of Wyoming. U. S. Geological Survey. Map scale 1: 500,000.
- 889 Love, J. D., Christiansen, A. C., and Ver Ploeg, A. J., 1992: Stratigraphic nomenclature chart for Wyoming.
890 Geological Survey of Wyoming Open-File Report 92-2. 1 sheet. Mahaney, W.C., 1978. Late Quaternary
891 stratigraphy and soils in the Wind River Mountains, western Wyoming. *In: W.C. Mahaney (Editor),*
892 *Quaternary Soils. Geoabstracts Ltd., Norwich, UK, 223-264.*
- 893 Mahaney, W.C., 1978. Late Quaternary stratigraphy and soils in the Wind River Mountains, western
894 Wyoming. *In: Mahaney, W.C. (Ed.), Quaternary Soils. Geoabstracts, Norwich, UK, pp. 233- 264.*
- 895 Mahaney, W.C., 1984a. Superposed Neoglacial and late Pinedale (Wisconsin) tills, Titcomb Basin, Wind
896 River Mountains, western Wyoming. *Palaeogeog. Palaeoclim. Palaeoecol.* 45, 149-63.
- 897 Mahaney, W.C., 1984b. Indian Basin advance in western and north-central Wyoming. *NW Sci.* 58, 94-102.
- 898 Makos, M., Rinterknecht, V., Braucher, R. Toloczko-Pasek, ASTER Team, 2018. Last glacial maximum and
899 Lateglacial in the Polish High Tatra Mountains – Revised deglaciation chronology based on the ¹⁰Be
900 exposure age dating. *Quat. Sci. Rev.* 187, 130-156.
- 901 Marcott, S.A., 2011. Late Pleistocene and Holocene Glacier and Climate Change. PhD Diss., Oregon St. Univ.
- 902 Masarik, J., Frank, M., Schaefer, J.M., Wieler, R., 2001. Correction of in-situ cosmogenic nuclide production
903 rates for geomagnetic field intensity variations during the past 800,000 years. *Geochim. Cosmochim.*
904 *Acta* 65, 2995-3003.
- 905 Masarik, L., Wieler, R., 2003. Production rates of cosmogenic nuclides in boulders. *Earth Planet. Sci. Lett.*
906 216, 201-208.
- 907 Mears, B., Jr., 1974. The evolution of the Rocky Mountain glacial model. *In: D.R. Coates (Ed.), Glacial*
908 *Geomorphology. Public. in Geomorph., State University of New York, Binghamton, 11-40.*
- 909 Menounos, B., Reasoner, M.A., 1997. Evidence for cirque glaciation in the Colorado Front Range during the
910 Younger Dryas chronozone. *Quat. Res.* 48, 38-47.
- 911 Miller, C.D. and Birkeland, P.W., 1974. Probable pre-Neoglacial age for the Type Temple Lake moraine,

- 912 Wyoming: Discussion and additional relative-age data. *Arct. Alp. Res.* 6, 301-306.
- 913 Monegato, G., Scardia, G., Hajdas, I., Rizzini, F., Piccin, A., 2017. The Alpine LGM in the boreal ice-sheets
914 game. *Scientif. Repts.* 7, 2078. doi:10.1038/s41598-017-02148-7.
- 915 Moss, J.H., 1949. Possible new glacial substage in the middle Rocky Mountains. *Geol. Soc. Am. Bull.* 60, 1972.
- 916 Moss, J.H., 1951. Late glacial advances in the southern Wind River Mountains, Wyoming. *Am. J. Sci.* 249,
917 865-883.
- 918 Munroe, J., Laabs, B., Shakun, J., Singer, B., Mickelson, D., Refsnider, K., Caffee, M., 2006. Latest Pleistocene
919 advance of alpine glaciers in the wouthwestern Uinta Mountains, Utah, USA: Evidence for the influence
920 of local moisture sources. *Geology* 34, 841-844.
- 921 Munroe, J.S. and Laabs, B.J.C., 2017. Combining radiocarbon and cosmogenic ages to constrain the timing of
922 the last glacial-interglacial transition in the Uinta Mountains, Utah, USA. *Geology* 45, 171-174.
923 doi:10.1130/G38156.1
- 924 Murphy, J.F. and Richmond, G.M., 1965. Geologic map of Bull Lake West, Wyoming. U.S. Geological Survey.
925 Map GQ-432, scale 1:24000.
- 926 NACSN (North American Committee on Stratigraphic Nomenclature), 1983. North American stratigraphic
927 code. *Am. Assoc. Petr. Geol. Bull.* 67, 841-875.
- 928 Nishiizumi, K., 2004. Preparation of ²⁶Al AMS standards. *Nucl. Instr. Meth B* 223-224, 388-392.
- 929 Nishiizumi, K., Imamura, M., Caffee, M.W., Southon, J.R., Finkel, R.C., McAninch, J., 2007. Absolute calibration
930 of ¹⁰Be AMS standards. *Nucl. Instr. Meth B* 258, 403-413.
- 931 Osborn, G., Clapperton, C., Davis, P.T., Reasoner, M., Rodbell, D.T., Seltzer, J.O., Zielinski, G., 1995. Potential
932 glacial evidence for the Younger Dryas event in the Cordillera of North and South America. *Quat. Sci. Rev.*
933 14, 823-832.
- 934 Osborn, G. and Gerloff, L., 1997. Latest Pleistocene and early Holocene fluctuations of glaciers in the
935 Canadian and northern America Rockies. *Quat. Int.* 38/39, 7-19.
- 936 Osborn, G., Clapperton, C., Davis, P.T., Reasoner, M., Rodbell, D.T., Seltzer, G.O., Zielinski, G., 1995. Potential
937 glacial evidence for the Younger Dryas event in the Cordillera of North and South America. *Quat. Sci.*
938 *Rev.* 14, 823-832.
- 939 Palacios, D., García-Ruiz, J.M., Andrés, N., Schimmelpfennig, I., Campos, N., Léanni, L., ASTER Team, 2017.
940 Deglaciation in the central Pyrenees during the Pleistocene-Holocene transition: Timing and
941 geomorphological significance. *Quat. Sci. Rev.* 162, 111-127. dx.doi.org/10.1016/j.quascirev.2017.03.007
- 942 Phillips, F.M., Zreda, M.G., Gosse, J.C., Klein, J., Evenson, E.B., Hall, R.D., Chadwick, O.A. and Sharma, P., 1997.
943 Cosmogenic ³⁶Cl and ¹⁰Be ages of Quaternary glacial and fluvial deposits of the Wind River Range,
944 Wyoming. *Geol. Soc. Am. Bull.* 109, 1453-63.
- 945 Pierce, K.L., 2004. Pleistocene glaciations in the Rocky Mountains. In: Gillespie, A.R., Porter, S.C., Atwater,
946 B.F. (Eds.), *The Quaternary Period in the United States*. *Dev. Quat. Sci.* 1, Jim Rose (Series Ed.). Elsevier,
947 Amsterdam, pp. 63-76.
- 948 Pierce, K.L., Licciardi, J.M., Good, J.M., and Jaworowski, Cheryl, 2018, Pleistocene glaciation of the Jackson

- 949 Hole area, Wyoming: U.S. Geological Survey Professional Paper 1835, 56 p.,
950 <https://doi.org/10.3133/pp1835>
- 951 Pigati, J.S., Lifton, N.A., 2004. Geomagnetic effects on time-integrated cosmogenic nuclide production with
952 emphasis on in situ ^{14}C and ^{10}Be . *Earth Planet. Sci. Lett.* 226, 193-205.
- 953 Rasmussen, S.O., Bigler, M., Blockley, S.P., Blunier, T., Buchhardt, S. L., Clausen, H.B., Cvijanovic, I., Dahl-
954 Jensen, D. Johnsen, S.J., Fischer, H., Gkinis, V., Guillevic, M., Hoek, W.Z., Lowe, J.J., Pedro, J.B., Popp, T.,
955 Seierstad, I.K., Steffensen, J.P., Svensson, A.M., Vallelonga, P., Vinther, B.M., Walker, M.J.C., Wheatley, J.J.,
956 Winstrup, M., 2014. A stratigraphic framework for abrupt climatic changes during the Last glacial period
957 based on three synchronized Greenland ice-core records: refining and extending the INTIMATE event
958 stratigraphy. *Quat. Sci. Rev.* 106, 14-28. [dx.doi.org/10.1016/j.quascirev.2014.09.007](https://doi.org/10.1016/j.quascirev.2014.09.007)
- 959 Refsnider, K.A., Laabs, B.J.C., Plummer, M.A., Mickelson, D.M., Singer, B.S., Caffee, M.W., 2008. Last glacial
960 maximum climate inferences from cosmogenic dating and glacier modeling of the western Uinta ice field,
961 Uinta Mountains, Utah. *Quat. Res.*, 69, 130-144, [doi:10.1016/j.yqres.2007.10.014](https://doi.org/10.1016/j.yqres.2007.10.014).
- 962 Richmond, G.M., 1948. Modification of Blackwelder's sequence of Pleistocene glaciation in the Wind River
963 Mountains, Wyoming. *Geol. Soc. Am. Bull.* 59, 1400-1401.
- 964 Richmond, G.M., 1957. Three pre-Wisconsin glacial stages in the Rock Mountain region. *Geol. Soc. Am. Bull.*
965 68, 239-262.
- 966 Richmond, G.M., 1964. Three pre-Bull Lake tills in the Wind River Mountains, Wyoming: A reinterpretation.
967 *U.S. Geol. Surv. Prof. Pap.* 501-D, 104-109.
- 968 Richmond, G.M., 1965. Glaciation of the Rocky Mountains. In: H.E. Wright, Jr. and D.G. Frey (Eds.), *The*
969 *Quaternary of the United States*. Princeton University Press, Princeton, NJ, pp. 217-230.
- 970 Richmond, G.M., 1973. Geologic Map of the Fremont Lake South quadrangle, Sublette County, Wyoming. U.S.
971 Geological Survey, Map GQ-1138.
- 972 Richmond, G.M., 1976. Pleistocene stratigraphy and chronology in the mountains of western Wyoming. In:
973 Mahaney W.C., (Ed.), *Quaternary Stratigraphy of North America*, Dowden, Hutchinson, and Ross,
974 Stroudsberg, PA, 353-379.
- 975 Richmond, G.M., 1986. Stratigraphy and correlation of glacial deposits of the Rocky Mountains, the
976 Colorado Plateau & the ranges of the Great Basin. *Quat. Sci. Rev.* 5, 99-127.
- 977 Richmond, G.M., 1987. Type Pinedale Till in the Fremont Lake area, Wind River Range, Wyoming. *Geol. Soc.*
978 *Am. Centennial Field Guide – Rocky Mtn. Sec.* 201-204.
- 979 Richmond, G.M. and Murphy, J.F., 1965. Geologic map of Bull Lake East, Wyoming. U.S. Geological Survey,
980 Map GQ-431, scale 1:24000.
- 981 Richmond, G.M. and Murphy, 1989. Preliminary Quaternary geologic map of the Dinwoody Lake area,
982 Fremont County, Wyoming. U.S. Geological Survey Open-File Rept, 89-435.
- 983 Rigual-Hernández, A.S., Colmenero-Hidalgo, E., Martrat, B., Bárcena, M.A., de Vernal, A., Sierro, F.J., Flores,
984 J.A., Grimalt, J.O., Henry, M., Lucchi, R.G., 2016. Svalbard ice-sheet decay after the Last Glacial
985 Maximum: New insights from micropalaeontological and organic biomarker paleoceanographical
986 reconstructions. *Palaeogeog. Palaeoclim. Palaeoecol.* 465A, 225-236.

987 Rood, D., Burbank, D. Finkel, R., 2011. Chronology of glaciations in the Sierra Nevada, California, from ^{10}Be
988 surface exposure dating. *Quat. Sci. Rev.* 30, 646-661.

989 Shakun, J.D., Carlson, A.E., 2010. A global perspective on Last Glacial Maximum to Holocene climate change.
990 *Quat. Sci. Rev.* 29, 1801-1816.

991 Shakun, J.D., Clark, P.U., Feng, H., Lifton, N.A., Zhengyu, L., Otto-Bliesner, B.L., 2015. Regional and global
992 forcing of glacier retreat during the last deglaciation. *Nat. Comm.* 21 Aug, 1-7. Doi:10.1038/ncomms9059

993 Shroba, R. R., 1989. Physical properties and laboratory data for soils formed in Pleistocene tills at Bull Lake,
994 Dinwoody Lakes, and Fremont Lakes, Fremont and Sublette counties, Wyoming. U.S. Geological Survey
995 Open-File Report OFR-89-370. 14 pp.

996 Stone, J., 2000. Air pressure and cosmogenic isotope production. *J. Geophys. Res.*, 105, 23753e23760.

997 Stuiver, M., Grootes, P. M. & Braziunas, T. F., 1995. The GISP2 d^{18}O climate record of the past 16,500 years
998 and the role of sun, ocean, and volcanoes. *Quat. Res.* 44, 341-354.

999 Thackray, Glenn D., 2008. Varied climatic and topographic influences on Late Pleistocene mountain
1000 glaciation in the western United States. *J. Quat. Sci.* 23, 671-681.

1001 Veggian, C.L., Smaglik, S.M., Dahms, D.E., 2010. Comparison of Unconsolidated deposits on areas of
1002 anomalous altitude and flatness in and around the Southern Wind River Basin, Fremont County,
1003 Wyoming. *Geol. Soc. Am. Abst. Programs* 42(5), 294.

1004 von Blanckenburg, F., Belshaw, N.S., O'Nions, R.K., 1996. Separation of ^9Be and cosmogenic ^{10}Be from
1005 environmental materials and SIMS isotope dilution analysis. *Chem. Geol.* 129, 93-99.

1006 Young, N., Briner, J., Leonard, E., Licciardi, J., Lee, K., 2011. Assessing climatic and nonclimatic forcing of
1007 Pinedale glaciation and deglaciation in the western United States. *Geology* 39, 171-174.

1008 Yu, Z. and Eicher, U., 2001. Three ampho-Atlantic century-scale cold events during the Bølling-Allerød
1009 warm period. *Géogr. Phys. et Quat.* 55, 171-179.

1010 Yu, Z. and Eicher, U., 1998. Abrupt climate oscillations during the last deglaciation in central North
1011 America. *Science* 282, 2235-2238.

1012 Zielinski, G.A. and Davis, P.T., 1987. Late Pleistocene age for the Type Temple Lake Moraine, Wind River
1013 Range, Wyoming, USA. *Geogr. Phys. Quat.* 41, 397-401.

1014 Zimmerman, S.G. Evenson, E.B. Gosse, J.C. Erskine, C.P., 1994. Extensive boulder erosion resulting from a
1015 range fire on the type-Pinedale moraines, Fremont Lake, Wyoming. *Quat. Res.* 42, 255-265.

1016 Züst, F., Dahms, D. Purves, R., Egli, M., 2014. Surface reconstruction and derivation of erosion rates over
1017 several glaciations (1 Ma) in an alpine setting. *Geomorphology*, 219, 232-247.

1018

1019 **Figure Captions**

1020 **Fig. 1.** Locations of the study area in North America and the Middle/ North Fork basins of the
1021 PopoAgie River system in the southeastern Wind River Range, including Stough Basin, Sinks
1022 Canyon and Cirque of the Towers. Detailed image from Landsat TM (Path 36, Row 30 (rgb),

1023 2% linear, 250k).

1024

1025 **Fig. 2.** Locations of the main upper-basin areas contributing ice to the trunk glaciers of the Middle
1026 and North Fork basins of the Popo Agie River system at the southeastern flank of the Wind
1027 River Range. The lower limit of each area approximates the confluence of the lowest cirque-
1028 valley ice stream with the canyon's trunk glacier. The ice-shed for the Middle Popo Agie
1029 system is ca. 149 km² while the ice-shed for the North Fork system is ca. 102 km². Note the
1030 locations of the Temple Lake and Alice Lake type localities. (Google Earth image).

1031

1032 **Fig. 3.** Oblique view of Table Mountain in relation to the mouth of Sinks Canyon and the
1033 allostratigraphic units of the Middle PopoAgie Basin noted in this study. Orange = Table
1034 Mountain diamicton; Solid yellow = units of Sacagawea Ridge till; Dotted yellow = isolated
1035 Sacagawea Ridge stagnant ice deposits within mapped Bull Lake boundary; Single yellow dots
1036 = isolated erratic boulders correlated to Sacagawea Ridge; Solid red = Bull Lake moraine and
1037 stagnant ice; Dashed red = assumed past limit of Bull Lake lateral moraine; Green
1038 solid/dashed = Pinedale moraine limit/purported past position. Red dots = location of
1039 boulders sampled for ¹⁰Be age analysis. HR1 & HR2 = locations of soil profiles noted in [Dahms](#)
1040 [\(2004a\)](#). Dashed orange lines = suggested kame terrace remnants on the NE of Table
1041 Mountain. (Google Earth image).

1042 Sampled boulders: TM1-6 = Table Mountain; ET1-2 = East Table Mountain; N1-3 = Nicholas
1043 Ranch; DS1 = Deer Spring. (Google Earth image).

1044

1045 **Fig. 4.** Vertical view of Sinks Canyon showing relations among previously mapped Sacagawea
1046 Ridge (yellow), Bull Lake (red) and Pinedale (green) moraine units ([Dahms, 2004a](#)) and
1047 isolated boulders sampled for ¹⁰Be exposure ages (yellow dots). Valley-side transects A and B
1048 indicated by white dots as locations of bedrock/boulder samples for ¹⁰Be and ²⁶Al exposure
1049 ages. (Google Earth image).

1050

1051 **Fig. 5.** (a) Details of Middle PopoAgie valley-side transects A-A' and (b) B-B' showing sample
1052 locations, sample numbers, and recalculated exposure ages ([Table 2](#)). All exposure ages are
1053 from polished-striated bedrock outcrops except triangles that designate samples taken from
1054 boulders (samples A-A', 97-110 and 97-117. Asterisk above age ranges designates that
1055 exposure ages are given as ¹⁰Be, ²⁶Al ages. Figure base modified from Figure 5 of [Fabel et al.](#)
1056 [\(2004\)](#).

1057

1058 **Fig. 6.** Oblique view of Stough Basin showing locations of Alice Lake (blue) and Temple Lake (red)

1059 moraines in Helen Lake and Bigfoot Lake cirques and associated locations of dated boulders.
1060 Cross-valley transects A-A' and B-B' are highlighted in orange. White dots indicate locations of
1061 bedrock samples for ^{10}Be and ^{26}Al exposure ages. Dotted white lines locate the mid-valley
1062 medial moraine (east) separating the Bigfoot Lake ice stream from the Helen Lake ice stream
1063 and the bedrock ridge (west) separating the Ice Lake from the Bigfoot Lake ice streams.
1064 Locations 97-90 and 97-91 are ^{10}Be -dated boulders on a remnant lateral moraine. (Google
1065 Earth image).

1066
1067 **Fig. 7.** Details of Stough Basin cross-valley transect A-A' (a) and B-B' (b) showing sample
1068 locations, sample numbers, and recalculated apparent exposure ages sampled from polished-
1069 striated bedrock exposures (Table 2).

1070
1071 **Fig. 8.** Vertical view of Cirque of the Towers showing major features of the cirque and the
1072 moraine units sampled for this study. Red = Temple Lake moraines; Blue = Alice Lake
1073 moraines; Yellow = medial moraine at the head of Lizard Head Meadows, between the glacier
1074 emanating from Cirque of the Towers and the glacier from Bear Lake. Black and white dots =
1075 locations of sampled boulders with associated sample numbers (Table 1). Note that the Alice
1076 Lake moraine south of Pingora Peak was not sampled but is included as the only other 'Alice
1077 Lake' moraine unit mapped here (Dahms et al., 2010). (Google Earth image).

1078
1079 **Fig. 9.** Summary of chronologies for Lateglacial-Holocene glacial activity in the Wind River Range
1080 [Fremont Lake Type Area (FLTA), Sinks Canyon, North Fork Canyon, Helen Lake, Bigfoot Lake,
1081 Temple Lake Type Locality (Marcott, 2011) and Titcomb Basin] normalized to the GISP2 2-m
1082 $\delta^{18}\text{O}$ record (Stuiver et al., 1995). Error bars approximate 1σ uncertainties. Grey dots
1083 represent individual ^{10}Be exposure ages from Alice Lake moraines; black dots represent
1084 individual exposure ages from Temple Lake moraines. Black triangles represent exposure
1085 ages from terminal moraines at the FLTA and Pine Bar Ranch; open triangles represent ages
1086 from moraines PD-2 and PD-3 in Sinks Canyon and moraines DP-1 and DP-2 in North Fork
1087 Canyon. Solid grey and black squares represent unweighted arithmetic averages of ages on
1088 moraine groups mapped as 'Alice Lake' and 'Temple Lake'. YD = Younger Dryas (GS-1 event of
1089 Rasmussen, et al., 2014); IACP = Intra-Allerød Cold Period; BA = Bølling/Allerød; OD = Oldest
1090 Dryas (GS-2.1a event of Rasmussen et al., 2014).

1091 Ages for the Fremont Lake Type Area (FLTA) and Titcomb Lake are from Shakun et al. (2015).
1092 Average ages for the SE Alps are generalized from Ivy-Ochs (2015; personal oral
1093 communication, 2016) and Böhlert et al. (2011). The age of Heinrich Event-1 is from
1094 Hemming (2004) and Rood et al. (2011).

Table 1

Exposure ages of moraine boulders, Middle and North Forks PopoAgie Basin, Wyoming.

Unit (<i>specification</i>)	Sample #	Latitude (°N)	Longitude (°W)	Elevation (m a.s.l.)	Sample thickness (cm)	Shielding factor	Erosion rate (mm ky ⁻¹)	¹⁰ Be Exposure Age (ka) ¹⁾
Table Mountain	Table Mtn-1	42.76	-108.76	2219	2.0	1.000	2.00	1397.3 ± 6903.6
	Table Mtn-2	42.76	-108.76	2219	2.0	1.000	2.00	149.1 ± 22.7 (14.5)
	Table Mtn-3	42.76	-108.76	2225	2.0	1.000	2.00	404.2 ± 97.2 (51.4)
	Table Mtn-4	42.76	-108.76	2227	2.0	1.000	2.00	199.1 ± 35.9 (26.2)
	Table Mtn-5	42.74	-108.77	2243	2.0	1.000	2.00	373.6 ± 95.1 (72.7)
	Table Mtn-6	42.74	-108.77	2253	2.0	1.000	2.00	Saturated
	East Table-1	42.76	-108.73	2225	4.0	0.993	2.00	429.6 ± 106 (44.7)
	East Table-2	42.76	-108.74	2225	3.0	1.000	2.00	235.3 ± 38 (16.4)
Sacagawea Ridge	Deer Spring	42.73	-108.81	2300	2.5	0.993	2.00	556.4 ± 187.7 (103.9)
Bull Lake <i>Outer Sinks Canyon</i>	Nicholas-1	42.46	-108.47	1783	2.0	0.921	2.00	126.6 ± 15.9 (5.3)
	Nicholas-2	42.46	-108.47	1780	3.0	0.999	2.00	163.3 ± 22.1 (7.5)
	Nicholas-3	42.46	-108.47	1777	3.0	0.963	2.00	92.6 ± 11.8 (6.1)
Pinedale <i>Lower Sinks Canyon</i>	Pinedale 2-1	42.74	-108.83	2083	2.5	0.980	0.00	19.7 ± 1.9 (0.5)
	Pinedale 2-2	42.74	-108.83	2086	3.0	0.983	0.00	21.4 ± 2.1 (0.7)
	Pinedale 2-3	42.74	-108.83	2086	2.5	0.983	0.00	21.8 ± 2.1 (0.6)
	Pinedale 3-1	42.74	-108.85	2168	1.5	0.973	0.00	18.7 ± 1.8 (0.3)
	Pinedale 3-2	42.74	-108.85	2174	2.5	0.977	0.00	20.1 ± 1.9 (0.5)
<i>North Fork Canyon</i>	Pine Bar-1	42.87	-108.90	1901	3.5	0.885	0.00	23.3 ± 2.3 (0.9)
	Pine Bar-2	42.87	-108.90	1901	2.4	0.959	0.00	22.5 ± 2.3 (0.9)
	Dickinson Pk1	42.81	-109.05	2623	2.8	0.994	0.00	26.9 ± 2.7 (0.9)

	Dickinson Pk2	42.81	-109.05	2624	0.6	0.994	0.00	16.4 ± 1.6 (0.6)
	CT7	42.78	-109.19	3086	3.2	0.943	0.00	17.6 ± 1.7 (0.5)
	CT8	42.78	-109.19	3086	2.0	0.950	0.00	14.8 ± 1.5 (0.6)
	CT9	42.78	-109.18	3062	2.0	0.982	0.00	14.9 ± 1.5 (0.5)
Temple Lake	Helen TL-1	42.64	-109.01	3399	3.0	0.962	0.00	13.9 ± 1.5 (0.7)
<i>Helen Lake cirque</i>	Helen TL-2	42.64	-109.01	3354	3.0	0.962	0.00	17.2 ± 1.7 (0.6)
<i>Cirque of the Towers</i>	CT1	42.77	-109.22	3216	2.5	0.947	0.00	15.8 ± 1.5 (0.5)
	CT2	42.77	-109.22	3214	3.2	0.954	0.00	15.1 ± 1.5 (0.5)
	CT5	42.73	-109.21	3125	3.0	0.972	0.00	15.1 ± 1.5 (0.5)
	CT6	42.73	-109.21	3125	2.2	0.972	0.00	16.1 ± 1.6 (0.5)
<i>Bigfoot Lake cirque</i>	MSCO - 001	42.64	-109.01	3347	2.0	0.946	0.00	12.8 ± 1.3 (0.6)
	MSCO - 002	42.64	-109.02	3355	2.0	0.946	0.00	14.9 ± 1.4 (0.4)
	MSCO - 003	42.64	-109.02	3355	2.0	0.946	0.00	15.6 ± 1.5 (0.5)
	MSCO - 004	42.64	-109.02	3355	2.0	0.943	0.00	14.5 ± 1.6 (0.8)
	MSCO - 005	42.64	-109.02	3355	2.0	0.946	0.00	15.3 ± 1.6 (0.7)
	MSCO - 006	42.64	-109.02	3355	2.0	0.946	0.00	13.9 ± 1.4 (0.4)
	MSCO - 007	42.64	-109.02	3363	2.0	0.946	0.00	13.1 ± 1.3 (0.5)
<i>Temple Lake Valley</i>	MTLO-01	42.72	-109.18	3253	2.0	0.981	0.00	15.7 ± 1.5 (0.4)
	MTLO-02	42.72	-109.18	3253	2.0	0.987	0.00	16.5 ± 1.6 (0.5)
	MTLO-03	42.72	-109.18	3253	2.0	0.985	0.00	15.8 ± 1.6 (0.5)
	MTLO-04	42.72	-109.18	3253	2.0	0.988	0.00	15.5 ± 1.5 (0.4)
	MTLO-05	42.72	-109.18	3253	2.0	0.988	0.00	14.8 ± 1.5 (0.6)
	MTLO-06	42.72	-109.18	3253	2.0	0.984	0.00	12.4 ± 1.2 (0.5)

	MTLO-07	42.72	-109.18	3253	2.0	0.987	0.00	14.3 ± 1.5 (0.7)
	MTLO-08	42.72	-109.18	3253	2.0	0.987	0.00	14.8 ± 1.6 (0.8)
Alice Lake	Helen AI-1	42.63	-109.01	3399	1.5	0.957	0.00	13.6 ± 1.5 (0.7)
<i>Helen Lake cirque</i>	Helen AI-3	42.63	-109.01	3398	2.0	0.944	0.00	12.7 ± 1.2 (0.3)
<i>Cirque of the Towers</i>	CT3	42.77	-109.22	3225	1.8	0.930	0.00	11.2 ± 1.1 (0.4)
	CT4	42.77	-109.22	3225	3.0	0.935	0.00	12.3 ± 1.3 (0.5)
<i>Bigfoot Lake cirque</i>	^M SCM - 01	42.64	-109.02	3370	2.0	0.937	0.00	12.2 ± 1.2 (0.3)
	^M SCM - 02	42.64	-109.02	3370	2.0	0.937	0.00	10.7 ± 1 (0.3)
	^M SCM - 03	42.64	-109.02	3370	2.0	0.935	0.00	9.6 ± 0.9 (0.3)
	^M SCM - 04	42.64	-109.02	3370	2.0	0.937	0.00	12.1 ± 1.2 (0.5)
	^M SCM - 05	42.64	-109.02	3370	2.0	0.937	0.00	12.2 ± 1.2 (0.3)
	^M SCM - 06	42.64	-109.02	3370	2.0	0.936	0.00	9.9 ± 1 (0.3)
	^M SCM - 07	42.64	-109.02	3370	2.0	0.937	0.00	10.2 ± 1 (0.4)

^Mdata from Marcott (2011)

¹⁾ age with 1 δ external and internal uncertainty

Table 2Exposure ages (^{10}Be and ^{26}Al) for bedrock transects and boulders, Middle Fork PopoAgie Basin.

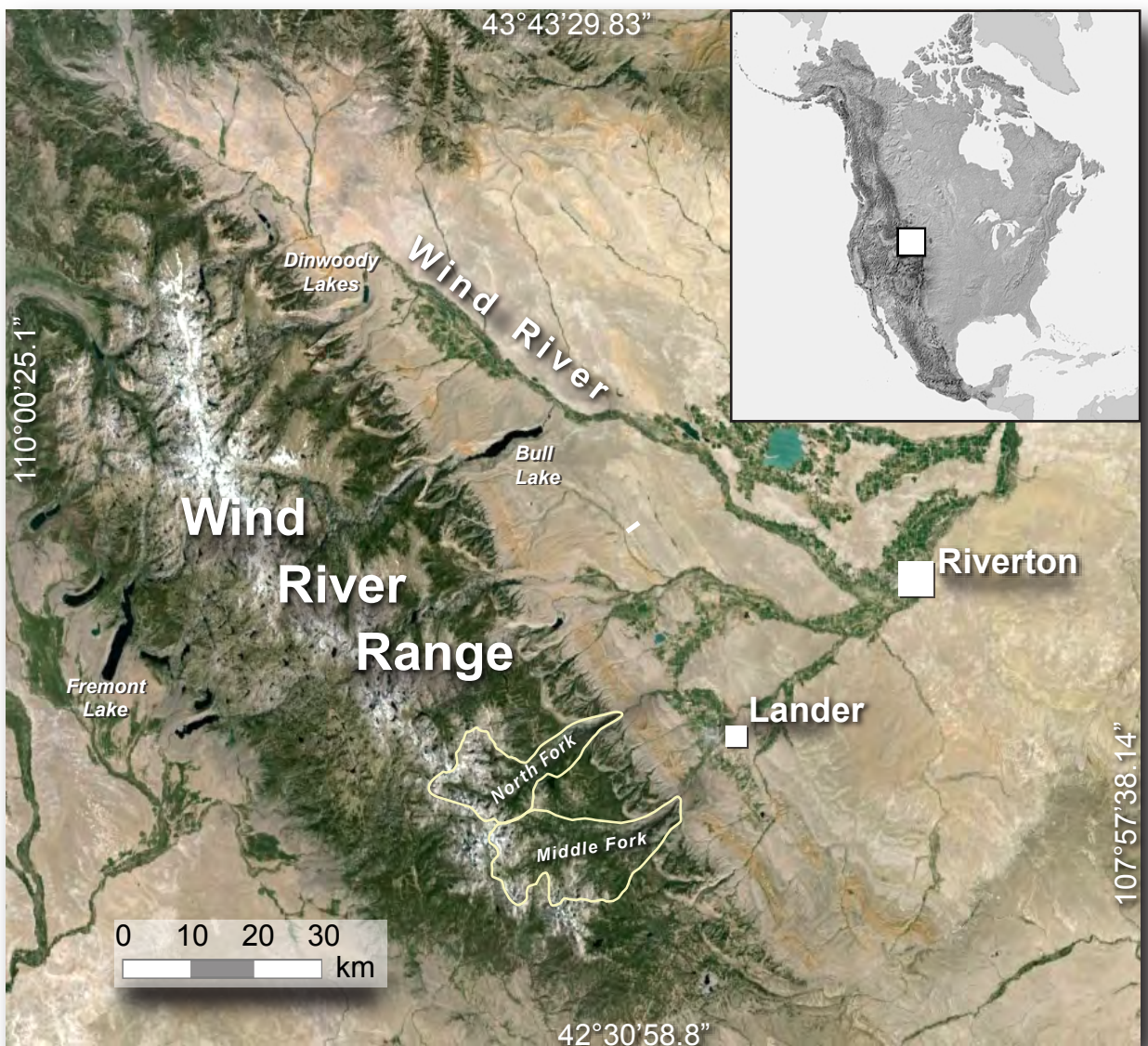
Unit	Sample #	Latitude (°N)	Longitude (°W)	Elevation (m a.s.l.)	Sample thickness (cm)	Shielding factor	Erosion rate (mm ky ⁻¹)	^{10}Be Exposure Age (ka) ¹⁾	^{26}Al Exposure Age (ka) ¹⁾	
Upper Sinks Canyon	A-97-108^	42.73	-108.90	2830	1	0.492	0.0	130.9 ± 13.7 (5.8)	114.5 ± 13.7 (8.4)	
	A-97-109	42.73	-108.90	2780	2	0.982	0.0	68.9 ± 6.9 (2.4)	54.8 ± 6.2 (3.6)	
	A-97-110b^	42.73	-108.90	2720	2	0.997	0.0	17.2 ± 2 (1.2)	16.2 ± 1.9 (1.2)	
	A-97-111^	42.73	-108.90	2680	1	0.997	0.0	21.2 ± 2.3 (1.1)	17.4 ± 2.3 (1.6)	
	Transect A	A-97-113^	42.73	-108.90	2650	1	0.979	0.0	17.5 ± 2 (1.2)	17.7 ± 2.1 (1.3)
		A-97-117b^	42.72	-108.90	2590	1	0.998	0.0		17 ± 2.1 (1.4)
		A-97-118^	42.72	-108.90	2560	1	0.965	0.0		15.1 ± 1.8 (1.1)
		A-97-120^	42.72	-108.90	2520	1	0.989	0.0		15.4 ± 1.7 (1)
Transect B	B-97-42^	42.73	-108.88	2560	2	0.998	0.0		63.2 ± 7 (3.7)	
	B-97-43^	42.73	-108.88	2530	1	0.525	0.0	123.1 ± 12.4 (4.3)		
	B-97-44^	42.73	-108.88	2500	5	0.972	0.0	92.4 ± 9 (2.2)		
	B-97-45^	42.73	-108.88	2480	1	0.991	0.0	98.7 ± 10.4 (4.8)	98.3 ± 10.9 (5.6)	
	B-97-46^	42.72	-108.88	2460	1	0.991	0.0	101.8 ± 10.9 (5.4)		
	B-97-47^	42.72	-108.88	2440	1	0.993	0.0	21.6 ± 2.5 (1.5)		
	B-97-48^	42.73	-108.88	2420	3	0.980	0.0	21.8 ± 2.6 (1.6)		
	B-97-49^	42.72	-108.87	2410	1	0.989	0.0	19.8 ± 2.5 (1.6)		
	B-97-85^	42.72	-108.88	2350	1	0.991	0.0	19.2 ± 2.6 (1.9)	18.4 ± 2.1 (1.3)	
	B-97-88^	42.72	-108.88	2450	2	0.986	0.0	19.6 ± 2.2 (1.2)		
Stough Creek Basin	97-100	42.65	-109.02	3460	2	0.985	0.0		27.3 ± 2.9 (1.5)	
	97-50	42.65	-109.19	3420	2	0.969	0.0	17.6 ± 1.8 (0.7)		
	97-52	42.65	-109.18	3390	2	0.970	0.0	18.4 ± 2 (1)		
	97-55	42.65	-109.01	3380	2	0.997	0.0	18.3 ± 1.8 (0.7)		
	Transect A	97-57	42.65	-109.15	3340	2	0.997	0.0	16.5 ± 1.7 (0.6)	
		97-59	42.65	-109.11	3300	2	0.983	0.0	17 ± 1.7 (0.7)	
		97-62	42.65	-109.00	3250	2	1.000	0.0	12.5 ± 1.3 (0.6)	
		97-63	42.65	-109.00	3280	2	1.005	0.0	13.5 ± 1.4 (0.6)	

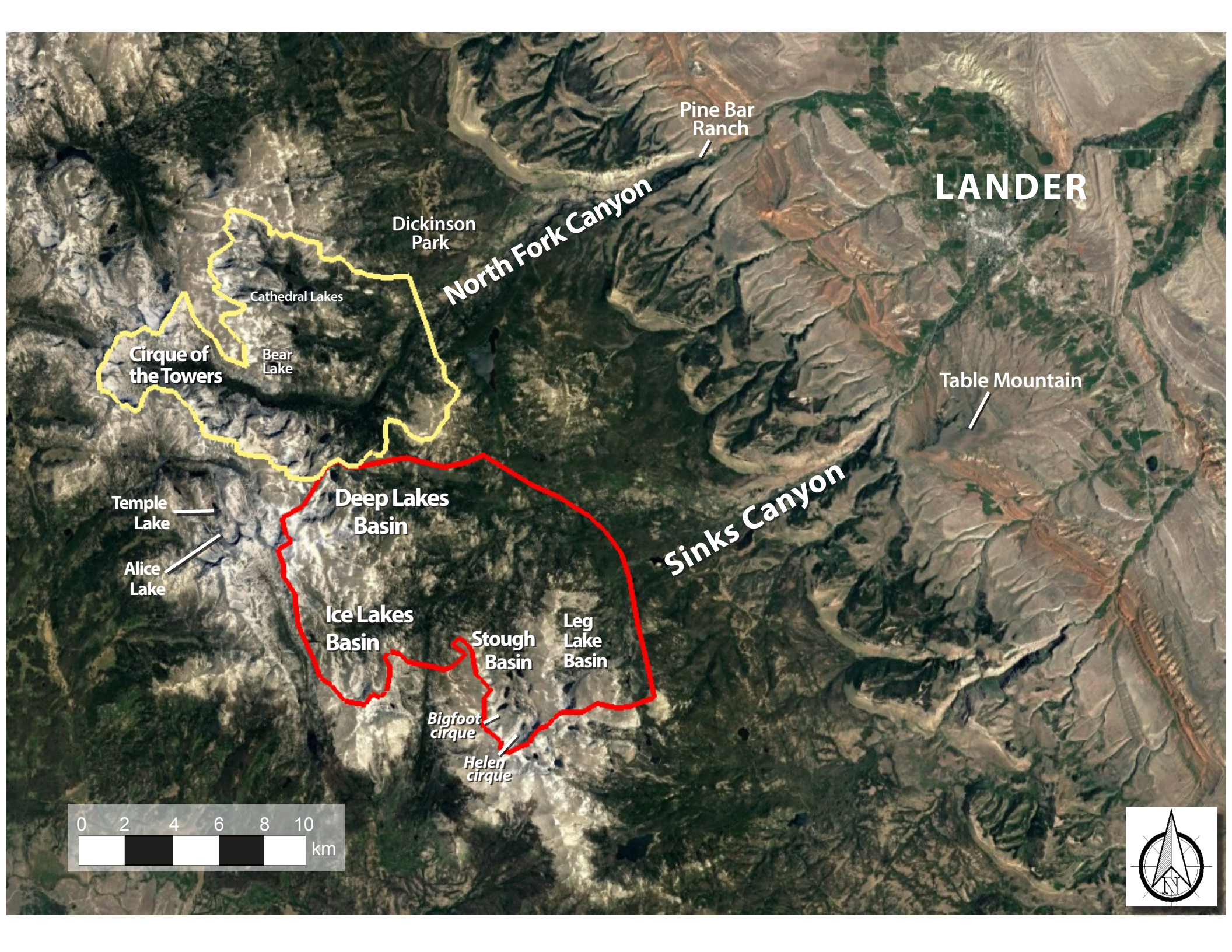
	97-66	42.65	-109.00	3330	2	1.011	0.0	14.8 ± 1.4 (0.4)
	97-68	42.65	-108.98	3350	2	1.016	0.0	17.9 ± 1.8 (0.6)
	97-75	42.64	-109.01	3390	2	1.022	0.0	18.5 ± 1.8 (0.6)
	97-76	42.64	-109.01	3370	2	1.028	0.0	16.9 ± 2.1 (1.4)
Transect B	97-78	42.64	-109.01	3330	2	1.033	0.0	16.1 ± 1.6 (0.6)
	97-80	42.64	-109.00	3290	2	1.038	0.0	17.6 ± 1.8 (0.7)
	97-97	42.65	-109.00	3320	2	1.044	0.0	14.7 ± 1.4 (0.4)
Stough Lateral moraine	97-90b	42.66	-109.00	3320	2	1.050	0.0	15.9 ± 1.6 (0.7)
	97-91b	42.65	-109.00	3330	2	1.055	0.0	16 ± 1.7 (0.8)

^ Original data published in Fabel et al. (2004)

b boulder

¹⁾ age with external and internal uncertainty





LANDER

North Fork Canyon

Sinks Canyon

Dickinson Park

Pine Bar Ranch

Table Mountain

Cirque of the Towers

Cathedral Lakes

Bear Lake

Deep Lakes Basin

Temple Lake

Alice Lake

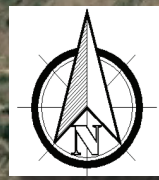
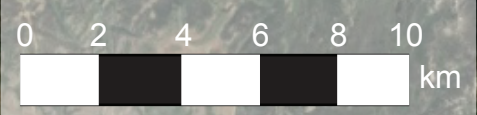
Ice Lakes Basin

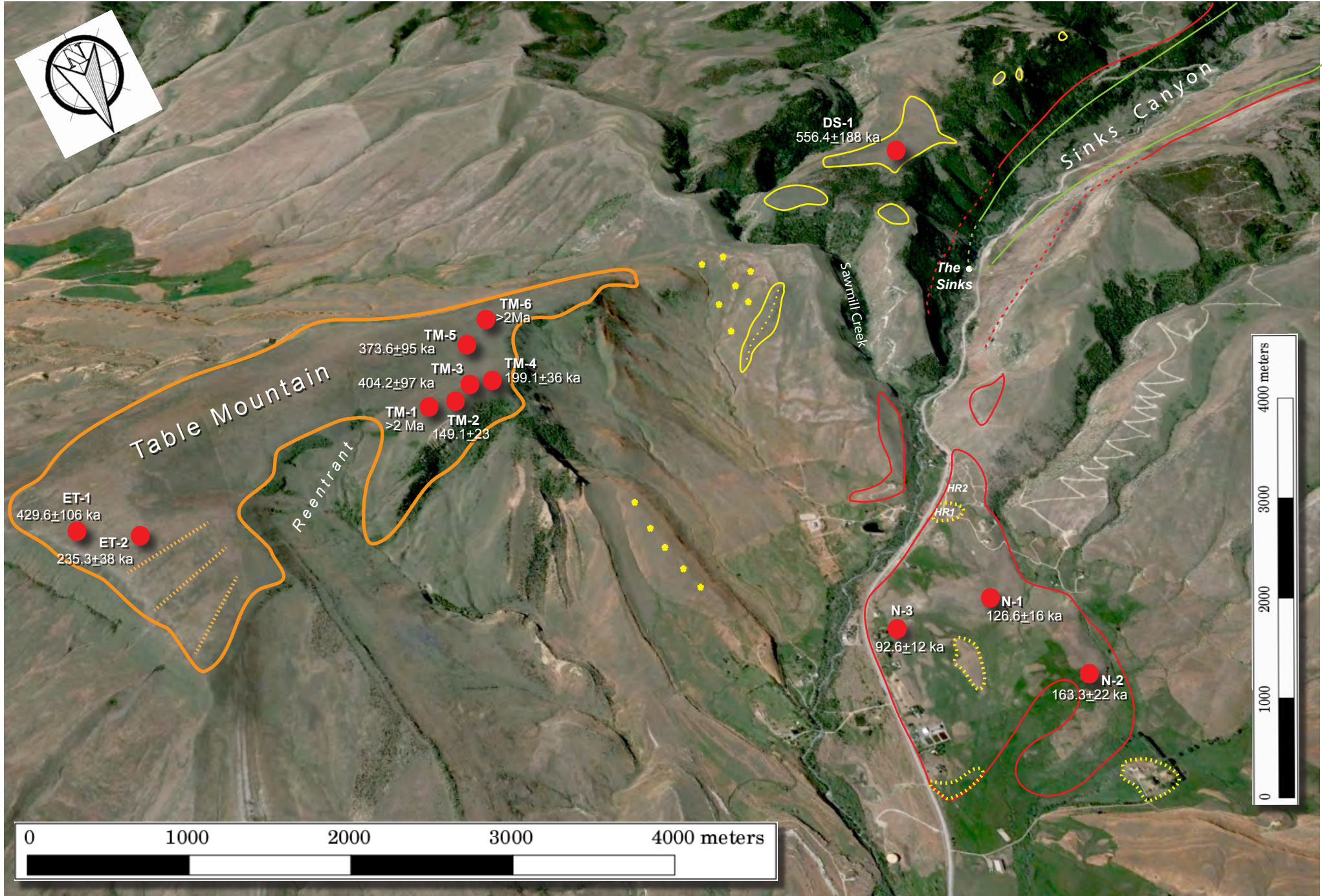
Stough Basin

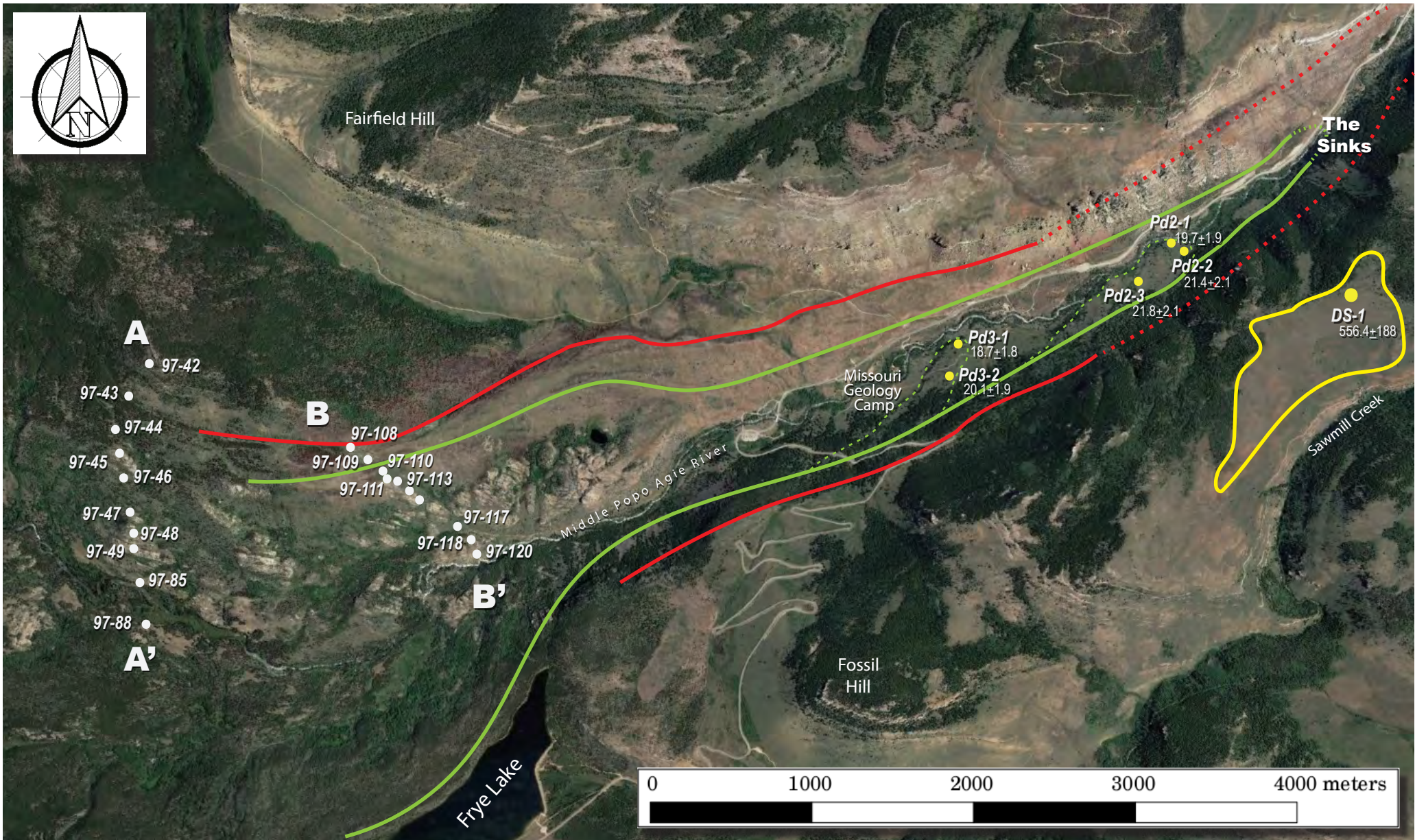
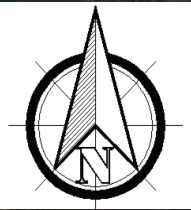
Leg Lake Basin

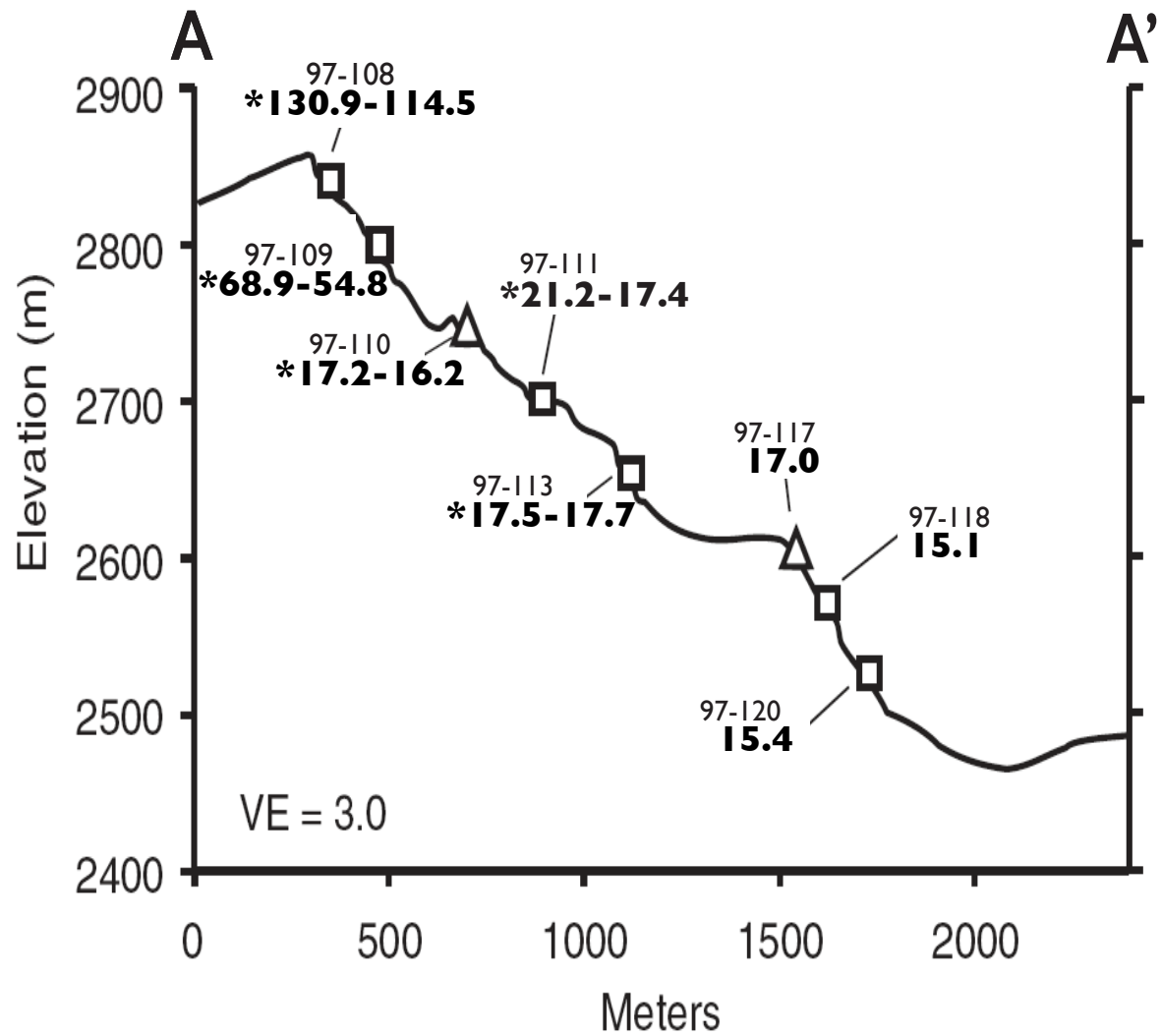
Bigfoot cirque

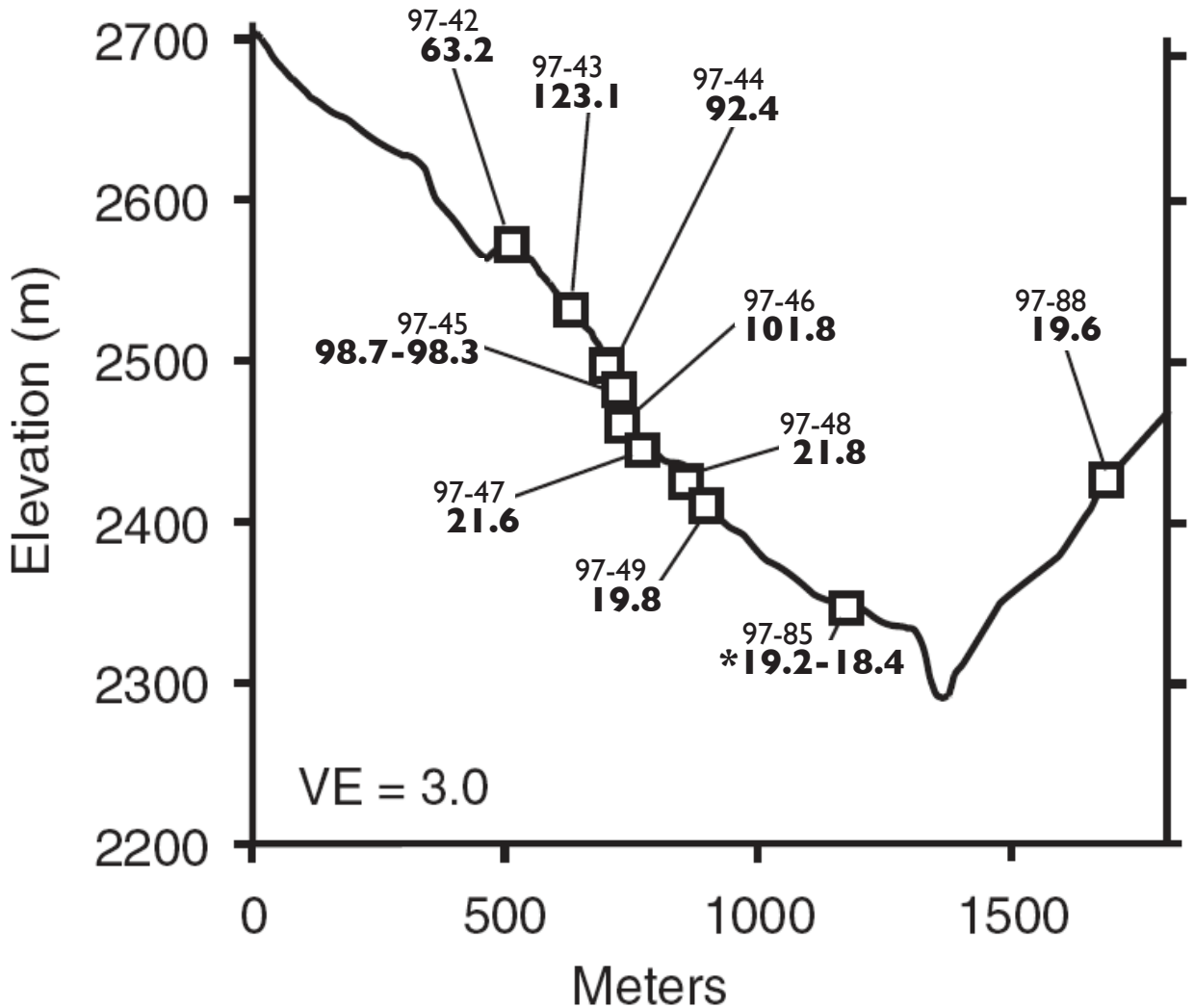
Helen cirque

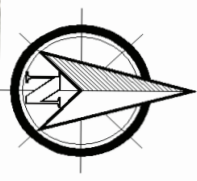








B**B'**



Roaring Fork Mountain

Roaring Fork Mountain

12.2±1.2
10.7±1.0
9.6±0.9
12.1±1.2
12.2±1.2
9.9±1.0
10.2±1.0

SCM-001-007*

SCO-001-007

12.8±1.3
14.9±1.4
15.6±1.5
14.5±1.6
15.3±1.6
13.9±1.4
13.1±1.3

13.6±1.5
AL-1

12.7±1.2
AL-3

TL-1
13.9±1.5

TL-2
17.2±1.7

Helen Lake

Bigfoot Lake
97-78

Wilhelm Lake

Ice Lake

A
97-100
97-50
97-52

B

97-75

97-76

97-80

97-97

B'

A'
97-68

97-55

97-57

97-59

97-62

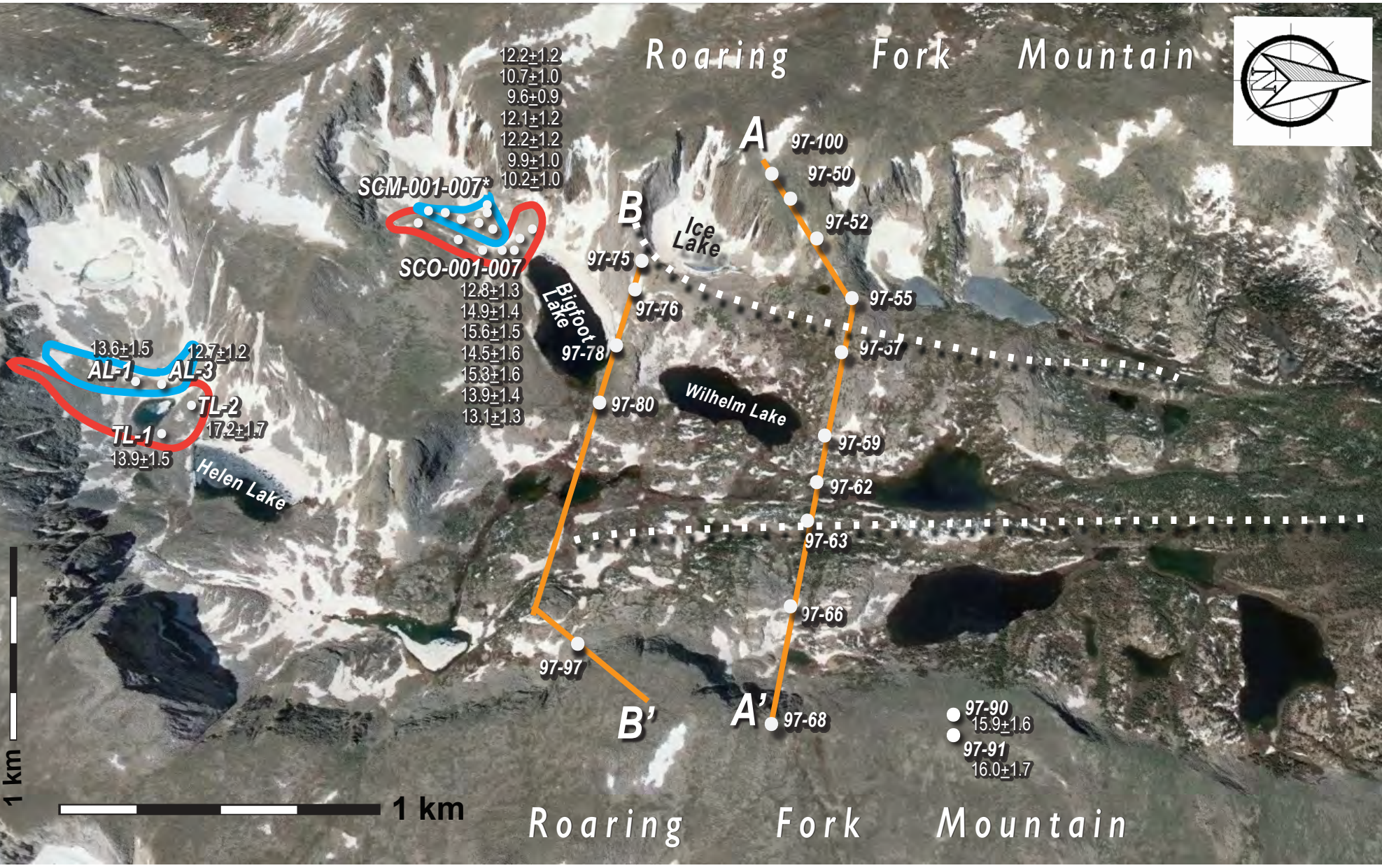
97-63

97-66

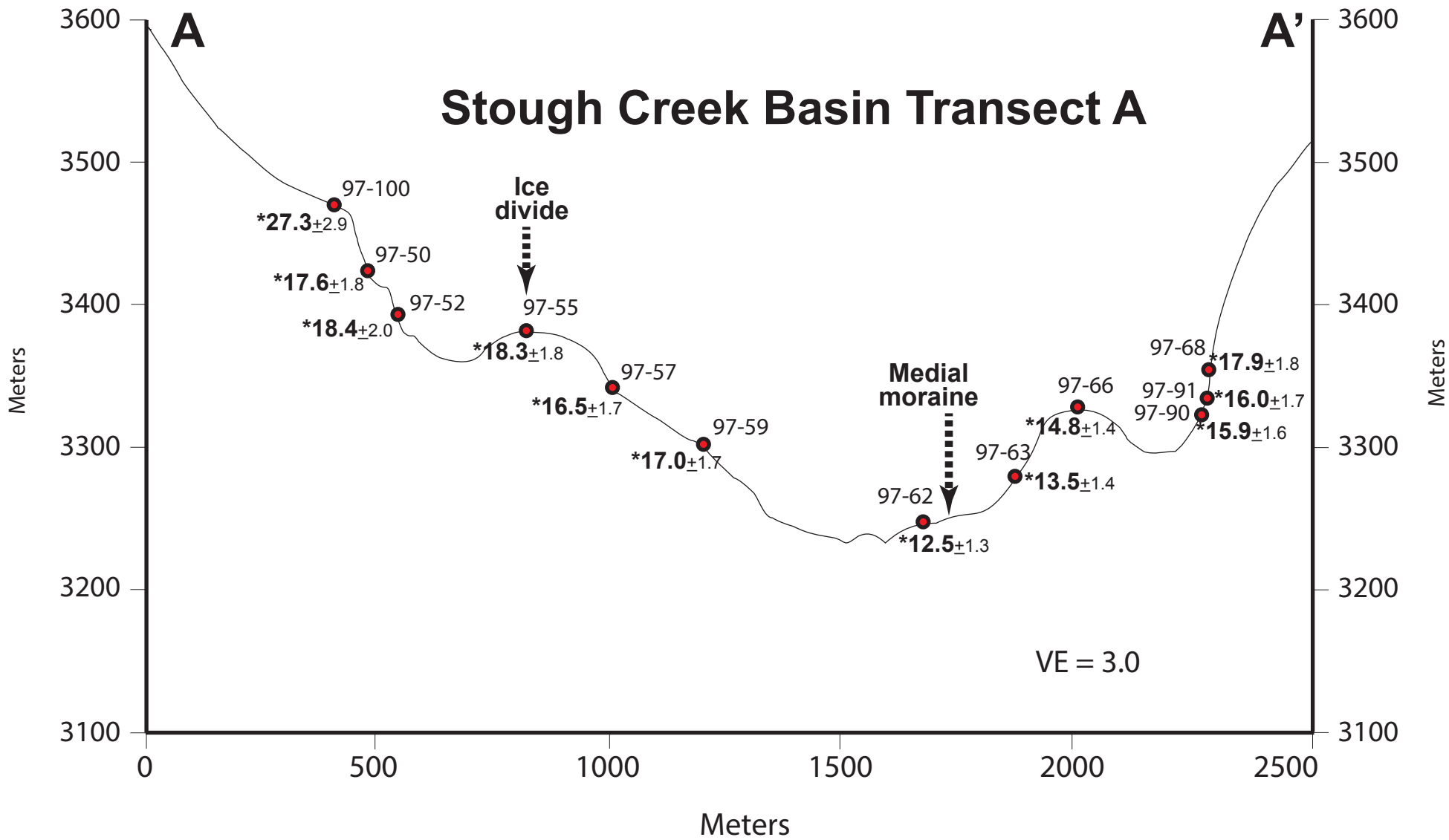
97-90
15.9±1.6
97-91
16.0±1.7

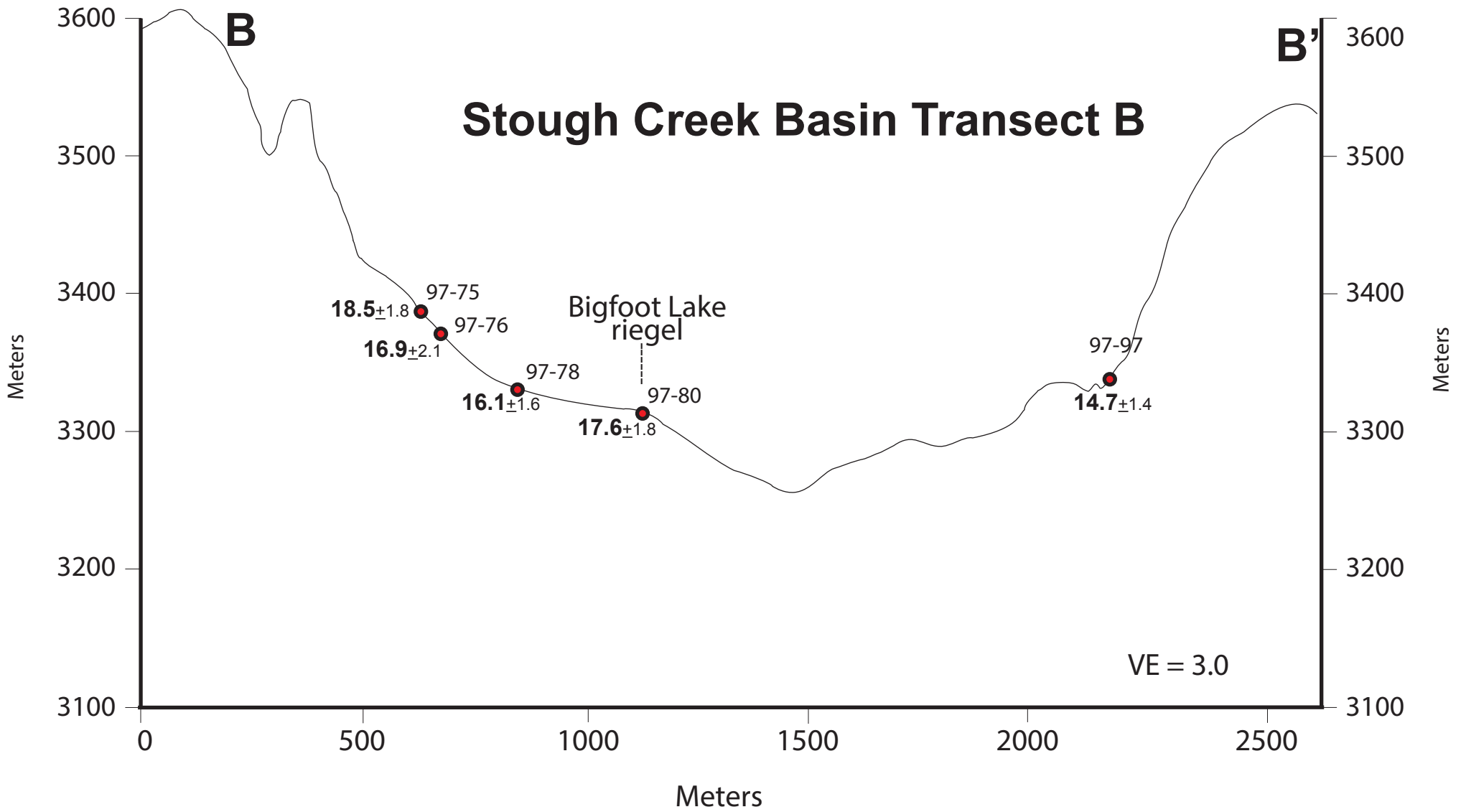
1 km

1 km



Stough Creek Basin Transect A





Cirque of the Towers

Pingora Peak

Lonesome Lake

Bear Lake

CT-4
12.3±1.3

CT-3
11.2±1.1

CT-1
15.8±1.5

CT-2
15.1±1.5

15.1±1.5

CT-5

CT-6

16.1±1.6

CT-7
17.6±1.7

CT-8

14.8±1.5

CT-9
14.9±1.5

Warbonnet Peak

Lizard Head Meadows

Google earth

1.6 km



